DRILLING OPTIMIZATION OF A CANEY SHALE WELL USING OFFSET WELL DRILLING DATA

By

DIONNE NYASHA MAYIBEKI

Bachelor of Science in Chemical Engineering

Oklahoma State University

Stillwater, Oklahoma

2019

Submitted to the Faculty of the
Graduate College of the
Oklahoma State University
in partial fulfillment of
the requirements for
the Degree of
MASTER OF SCIENCE
December, 2021

DRILLING OPTIMIZATION OF A

CANEY SHALE WELL USING OFFSET WELL

DRILLING DATA

Thesis Approved:

Dr. Geir Hareland

Thesis Advisor

Dr. Mohammed Al Dushaishi

Dr. Prem Bikkina

ACKNOWLEDGEMENTS

I would like to thank my advisor and supervisor Dr. Geir Hareland for his dedication, immense knowledge, and supervision during the last two years. My sincere heartfelt gratitude and appreciation to a wonderful supervisor for providing me with the guidance and counsel I need to succeed in the Master program. Sincere appreciation to my parents (Lucas Mayibeki and Priscilla Mayibeki) and sister (Deseree Mayibeki) for their endless love and support, as nothing would have been possible without them. I would like to thank my brilliant committee members Dr. Prem Bikkina and Dr. Mohammed Al Dushaishi. Their help both professionally and personally has helped me to fulfill my requirements. A special thank you to Haden Kolmer, Jordon Massey, and Nicolai Kjeldal for all your help, knowledge, and contributions. I would also like to extend my gratitude to the Department of Energy and Continental Resources for providing the funding necessary for this research to be possible.

Name: DIONNE NYASHA MAYIBEKI

Date of Degree: DECEMBER, 2021

Title of Study: DRILLING OPTIMIZATION OF A CANEY SHALE WELL USING OFFSET WELL DRILLING DATA

Major Field: PETROLEUM ENGINEERING

Abstract: Cost reduction can be achieved by utilizing drilling simulators to efficiently optimize new wells to be drilled using available adjacent or offset well drilling data. Different approaches involving simulators that use inverted rate of penetration (ROP) models have been implemented to help improve the drilling performance of wells primarily within the Caney shale. A complete simulation and optimization technique is presented herein which utilizes drilling data from a nearby or offset well (Garrett well) to create an optimized drilling program for a new well to be drilled (Gallaway well). The Pason Drilling Simulator (PDS), previously known as DROPS® was used in this research to obtain an optimized drilling program for the Gallaway well. The PDS software uses inverted ROP models for different bit types, reported bit wear, lithological information, and pore pressure in addition to the drilling parameters. Raw drilling data from the offset well consisted of ROP, revolutions per minute (RPM) and mud weight among other drilling variables. Along with the PDS, the D-WOB software was run on the Garrett well drilling data to obtain the depth-based drill string friction coefficient and downhole weight on bit (DWOB) for every foot of the drilled well which is needed as an input into the PDS. The DWOB was analyzed, and results were compared to the SWOB to show the effect of wellbore friction on the weight-on-bit under downhole conditions. The results proved that the DWOB is significantly less than SWOB in the directional section of the well due to frictional losses along the wellbore. Several PDS simulations using the apparent rock strength logs (ARSL) and the concept of the learning curve were applied to define the optimum drilling parameters for the Gallaway well. To verify the accuracy of the PDS software, the simulation results will later be compared to results from actual field data from the Gallaway well by overlaying the ARSLs, the simulated ROP against the actual, and by analysis and observation of the trend displayed by plotting depth versus the unconfined rock strengths (UCS) of both wells in the different formations. The D-Series software will be used to obtain the ARSL for the drilled Gallaway well.

TABLE OF CONTENTS

Chapter Page

LIST OF TABLES

Table Page

LIST OF FIGURES

Figure Page

Figure Page

NOMENCLATURE

ΔBG	change in bit tooth wear
Δp	pump-off force acting on the face of the bit
μ	mud plastic viscosity (cp)
a, b, c	bit coefficients
a_c, b_c, c_c	chip hold-down coefficients
a_d, b_d, c_d	drag bit lithology coefficients
A_p	pump-off area (in^2)
A_r	relative abrasiveness
a_s, b_s	rock strength lithology coefficients
A_v	front projected area of each diamond
A_{vw}	projected area of the worn section of a diamond
BHA	bottom hole assembly
C_a	drag bit wear coefficient
C_b	bit cost ($/ft)
CCS	confined compressive strength (ksi)
C_f	cost per foot ($/ft)
C_m	downhole motor cost ($/hr)
Corr	lithology correction factor
C_r	rig cost ($/hr)
D	depth drilled (ft)
D_{bit}	bit diameter (in)
$D_{nozzles}$	diameter of nozzles (1/32 in)
D_s	diameter of diamond stones (in)
DWOB	downhole weight-on-bit (klbf)
F_c (P_e)	chip hold-down function
GDL	geological drilling log
GPM	pump flow rate (gpm)
GPM	mud flow rate (gpm)
IADC code	bit classification
I_m	modified jet impact force (lbs)

KA	bit apparent nozzle area (in^2)
LWD	logging while drilling
MD	measured depth (ft)
MW	mud weight (ppg)
MWD	measurement while drilling
LWD	logging while drilling
NDB	natural diamond bit
N_s	number of diamond stones
P	diamond penetration (in)
PDC	polycrystalline diamond compact bit
PDS	pason drilling simulator
P_w	diamond penetration with wear (in)
P_w	penetration loss due to wear of diamond
R_e	equivalent bit radius (in)
ROP	rate of penetration (ft/hr)
RPM	revolutions per minute
S	confined rock strength (psi)
S_o	unconfined rock strength (psi)
SWOB	surface weight-on-bit (klbf)
T_c	connection time (hr)
T_r	rotating time (hr)
T_t	trip time (hr)
TVD	true vertical depth (ft)
UCS	uniaxial compressive strength (ksi)
V_d	volume worn by each cutter per bit revolution
W_f	wear function
WOB	weight-on-bit (klbs)
$WOB_{applied}$	applied weight-on-bit
WOB_{mech}	mechanical weight-on-bit (klbs)
ρ	mud density (ppg)
a_1,b_1,c_1	drill bit constants
a_s,b_s,a_e,b_e	formation constants obtained from regression analysis
B_x	function of drill bit properties
D_b	diameter of bit (in)
E	Young's modulus
F_t, F_b	force or hook load at top and bottom, respectively (klbf)
F_n	net normal force acting on the drill string element (klbf)
h_x	hydraulic efficiency function
K	empirical constant in ROP model
K_p	permeability (darcy)
K_s	sliding model constant
ΔL	element length of drill string (ft)
W_f	buoyed weight (klbf)

β	buoyancy factor
μ	coefficient of friction
$\emptyset$	porosity
θ	dogleg angle (°/100ft)
α_t, α_b	inclination at top and bottom respectively (°)
ϕ_t, ϕ_b	azimuth at top and bottom respectively (°)
[C]	damping matrix
[k]	stiffness matrix
[M]	mass matrix
F_n	normal force (klbf)
F_f	friction force (klbf)
F_t	tension or compression in drillstring
$\Delta\alpha$	increment of azimuth (°)
$\Delta\Theta$	increment of inclination (°)
W	weight of element (lbf)
$\{U\}$	generalized displacement vector
$\{\dot{U}\}$	generalized velocity vector
$\{\ddot{U}\}$	generalized acceleration factor
$\{F\}$	force vector
A_B	bit face area (ft^2)
a_3, b_3	empirical constants
a_1, b_1, c_1	empirical constants
a_2, b_2, c_2	empirical constants
ABR	abrasiveness constant
BR	PDC cutter back rake angle (°)
b(x)	function for the effect of number of blades
Ca	bit wear coefficient
e	individual sheave efficiency
F_{top}	tension on the top of each drill string element
F_{bottom}	tension on the bottom of each drill string
h(x)	hydraulic efficiency function
HHP	hydraulic horsepower (hp)
HSI	horsepower per square inch
JSA	junk slot area (in^2)
K_I	empirical constant
N_b	number of blades
n_{lines}	number of lines between blocks
P_B	bit pressure drop (psi)
Q	pump flow rate (gpm)
SR	PDC cutter side rake angle (°)
T_{dh}	downhole torque (klbf·ft)

V_p	compressional velocity (ft/s)
V_s	shear velocity (ft/s)
w	unit pipe weight (lb/ft)
W_f	bit wear function
α	inclination angle (°)
v	Poisson's ratio
ΔBG	cumulative bit wear
Δp	differential pressure (psi)
Δt_c	compressional travel time (s)

CHAPTER I

INTRODUCTION

1.1 Overview

The constant need to reduce oil exploration and development costs is inevitable. Drilling costs can represent as much as up to 40% of the entire exploration and development costs (Hossain, 2015). As a result, there is an increasing demand for drilling simulators and artificial intelligence technology in the drilling industry to simulate and optimize oil and gas wells for efficiency and cost-effective drilling. Various strategies to optimize a well have been developed, including the torque-on-bit (TOB) response which is used to reduce vibrations at the bit or mechanical specific energy (MSE) in order to reduce the energy used by the bit (Hegde and Gray, 2018). (Eren and Ozbayoglu, 2010) developed a model that uses actual field data collected through modern well monitoring and data recording systems to predict the ROP as a function of available parameters. Although the concept of drilling is the same globally, numerous factors can influence a wider range in drilling costs and performance. Most industries have sought to include futuristic methods of technology by using simulators and optimizers to cut costs and improve the efficiency curve. With the help of drilling simulators, a preplanned analysis that accounts for costs, lithology and other drilling variables is outlined before the actual drilling takes place. This gives the driller a glimpse into the actual drilling procedure before it has occurred, thus allowing for any adjustment

Various drilling parameters such as lithology, bit type, downhole conditions, circulation system and drilling mud bit hydraulics have major influence on drilling costs and efficiency. The formation geology at the site and the location of the target reservoir are also primary factors that influence drilling cost. Geologic formations vary across the world, and indeed, within the same

producing basin. Hard, abrasive, and heterogeneous formations typically have low penetration rates, frequent drill string failures, and significant deviation from the planned trajectory which can cause delays in drilling and equipment failure. Artificial intelligence and simulation technology can optimize and simulate wells in the most remote areas and complicated geological formations and the data can be used to plan for new wells.

The incorporation of all these challenging features brings the frontier thought for current and future researchers. Simulation technology has proven to be reliable and accounts for wells drilled in more-hostile environments, more-complex well programs, and deeper wells (Lummus, 1970).

1.1 Research Objectives

The first objective of this research is to shed light on the Pason Drilling Simulator (PDS) by using drilling data from an existing offset well (Garrett well) to create a complete optimized drilling program for an upcoming well (Gallaway well) to be drilled by Continental Resources (CLR). To achieve this objective, the friction coefficient, and Down Hole Weight on Bit (DWOB) must be obtained using the D-WOB software, as the PDS requires accurate DWOB values to generate the apparent rock strength log (ARSL). The ARSL from the Garrett well is then adjusted to the Gallaway well by stretching and shrinking the formation to match the proposed formation tops for the Gallaway well. The casing points are then inserted in to the PDS and different bits and operating parameters are simulated. The trial and run procedure results in a simulator learning curve and the best results within the equipment limitations given by CLR have been presented to CLR prior to the drilling of the Gallaway well. The final objective is to obtain field data from CLR after the Gallaway well has been drilled and will be presented once the drilling data is made available from

CLR. With this data, the D-series software will be run to obtain DWOB, which will be used to generate the ARSL for the Gallaway well. A comparison between the modified Garrett ARSL and the ARSL generated by the D-Series software and the PDS from Gallaway drilling data can then be made by overlaying the ARSLs analyzing any discrepancies or similarities. The simulated and the actual ROPs from the two wells will also be compared and analyzed.

1.2 Thesis Structure

Chapter 2 presents a brief study on the history and evolution of simulation and optimization technology within the drilling industry, which was first applied in 1967 (Lummus,1970) along with a detailed literature review on some drilling variables and drilling simulators that have been developed in the past. Chapter 2 also introduces the ROP models that are used in some of the simulators to calculate apparent rock strength (ARS). The effect of wellbore friction along with some torque and drag models used to calculate wellbore rotary friction and wellbore sliding friction are also explained in this chapter. Literature review on the D-series software, which consists of two software applications (D-WOB and D-ROCK) is also mentioned and explained in this chapter and will be used to calculate the friction coefficient and DWOB from surface weight on bit (SWOB) for the Garrett well, and to generate an ARSL using field data from the well. The model used by the D-WOB software to calculate the friction coefficient is also explained in this Chapter 2. Chapter 3 presents information on the Garrett well. The Garrett well is the offset well used throughout this thesis study and information including the well path, location and geological setting on the Garrett can be found in Chapter 3. Chapter 4 presents the research materials and describes the research methodology. The purpose of this chapter is to introduce the input parameters along with the simulation steps that were undertaken to calculate the friction coefficient and DWOB for the Garrett well and produce an optimized drilling program for the Gallaway well using the PDS. Chapter 5 presents the results obtained from the simulator, including the finalized drilling program for the Gallaway well. The generated strength log from the simulator is also presented along with

detailed sectional optimization results. Along with the simulated results, this chapter also shows the results obtained from the D-WOB software for the Garrett well. The friction coefficient and DWOB results from the D-WOB software are all described and explained in this chapter. A discussion section is also included in this chapter which explains simulation and optimization alternatives that were carried out in an effort to increase drilling efficiency. To conclude this chapter, a recommendation based solely on the optimization process using the PDS software was drawn and recommended for the Gallaway drilling operation. A full comparison of a fully optimized Gallaway ARSL and the ARSL generated from Gallaway drilling data using the D-Series software can later be analyzed for similarities and differences in UCS values when the drilling data has been provided by CLR. Chapter 6 outlines the conclusions of this thesis study and Chapter 7 provides suggestions for future work and research.

CHAPTER II

REVIEW OF LITERATURE

2.1 Background

Optimized drilling has come a long way, thanks to numerous researchers who have spent considerable time studying the effects of drilling variables and how they relate to each other. Optimized drilling techniques, first applied in 1967, have significantly reduced drilling costs (Lummus, 1970). The development of rotary drilling can be split into four distinct periods; Conception, Development, Scientific and Automation periods, with the most productive years falling under the Scientific period, dating from 1958 to 1968 (Lummus, 1970). Table 1 displays some of the detailed accomplishments of these periods from 1900 to 1968, with optimized drilling being one of the most significant accomplishments of the Scientific Period.

According to Lummus (1970), the lowest cost of drilling results when limits are imposed that maximize not only drilling rate, but also equipment use and wellbore stability. In many cases, some drilling variables are limited or lowered to maximize others. A balance program is usually developed where drilling variables are at their most effective level. The philosophy of drilling optimization relies on using the record of the first well as a basis for calculations and applying optimization techniques to the upcoming wells (Lummus, 1970).

Geomechanical data can also be obtained with logging operations performed in the wellbore, but these tools are typically expensive and have delicate components that can increase the risk of failure while performing operations. Through recent years, models have been developed and software has been utilized to evolve the MWD and LWD values into reputable correlations for rock strength. A convenient ROP model was developed to calculate rock mechanical properties such as confined compressive strength (CCS) and UCS at each drilled depth from drilling data such as ROP, weight on bit (WOB) and revolutions per minute (RPM) (Hareland and Nygaard, 2007). These models can enable drilling and completion optimization to take place without the increased cost of LWD or MWD tools.

Table 1: Rotary Drilling Development (Lummus, 1970)

Period	**Date**	**Development**
Conception	1900-1920	Rotary drilling principle,1900 (spindletop) Rotary bits, 1908 (Hughes) Casing and cementing, 1904-1910 (Haliburton) Drilling mud, 1914-1916 (National Lead Co.)
Development	1920-1948	More powerful rigs Better bits Improved cementing Specialized muds
Scientific	1948-1968	Expanded drilling research Better understanding of hydraulic principles Significant bit improvements Optimized drilling Improved mud technology
Automation	1968	Full automation of rig and mud handling “Closed-Loop” computer operation of rig Control of drilling variables Complete planning of well drilling from spud to production

2.2 Drilling Variables

Lummus (1970) studied the effect of drilling variables and how they interact with one another. According to Lummus, drilling variables can be grouped as alterable or unalterable as depicted in Table 2. Some unalterable variables may be altered by changing the alterable ones. For instance, a change in mud type may allow for a change in bit type resulting in a faster penetration rate through a particular formation. In considering which variables to choose for mathematical optimization, experience and research suggest four alterable and two unalterable variables as listed in Table 3 (Lummus, 1970). When variables are individually or simultaneously increased from one level to another, responses may produce a negative or positive interaction. A negative interaction exists when an increase in two drilling variables fails to produce a higher drilling rate as expected while a positive interaction produces a higher drilling rate than expected when two variables are increased (Lummus, 1970). Table 4 illustrates interactions among some important drilling variables and these results may change if the levels at which the variables are being compared are changed. Figure 1 shows the related responses in the drilling rate when the variables are increased from one level to another.

Table 2: Drilling Variables (Lummus, 1970)

Alterable	Unalterable
Mud • Type • Solids Content • Viscosity • Fluid Loss • Density Hydraulics • Pump Pressure • Jet Velocity • Circulating Rate • Annular Velocity Bit type Weight-on-bit Rotary speed	Weather Location Rig conditions Rig flexibility Corrosive borehole gases Bottom-hole temperature Round-trip time Rock properties Characteristic hole problems Water availability Formation to be drilled Crew efficiency Rock properties Characteristic hole problems Formation to be drilled Crew efficiency Depth

Table 3: Variables Considered in Optimization (Lummus, 1970)

Alterable	Unalterable
Mud Hydraulics Bit type Weight-rpm	Formation to be drilled Depth

Table 4: Typical Drilling Variable Interaction in Hard Rock (Lummus, 1970)

Variable Combination	**Interaction**
Weight-rpm	Negative
Weight-hydraulics	Positive
rpm-hydraulics	None
Low solids-hydraulics	Positive
Low solids-weight	Positive
Bit type-formation	Either
Low solids-bit type	Positive
Rpm-formation	Negative
Mud Solids-NDP*	Positive
*Nondispersed, dual-action polymer	

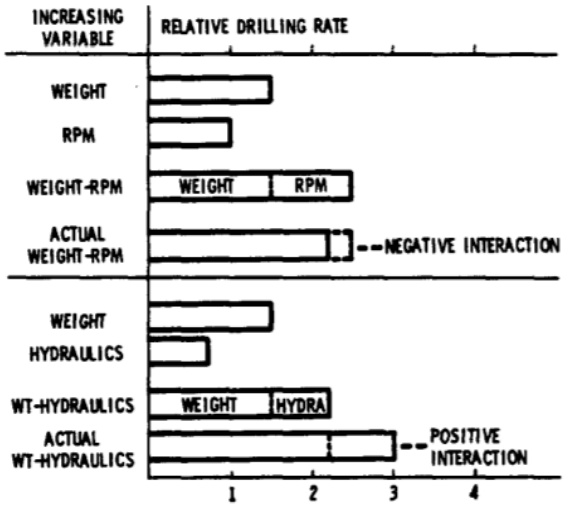

Figure 1: Positive and Negative Interactions (Lummus, 1970)

2.3 The Drilling Simulator

Drilling simulators have proven to be powerful tools, with the capacity for reproducing the drilling performance observed in drilled wells. Simulators have made it possible to use drilling data from reference or offset wells to simulate a new well to be drilled entirely from simulation results.

Utilizing simulators has proven to show a significant reduction in cost and time, and can be helpful in the preplanning analysis for new wells to be drilled using different bit types and designs (Hareland and Nygaard, 2007). Through recent years, models have been developed and software has been utilized to evolve the measurement while drilling (MWD) or logging while drilling (LWD) values into reputable correlations for rock strength. This will further enable drilling and completion optimization to take place, without the added cost of LWD or MWD tools.

2.3.1 Engineering Simulator for Drilling (ESD)

In 1981, (Millheim, 1983) started creating the ESD software which works by subdividing the drilling system into parts consisting of geology, wellbore, drilling rig, fluid system and drill string, as shown in Figure 2. The ESD software was created to be a self-instructional system that can be mastered in less than a day without any prior knowledge of computers (Millheim, 1983). Figure 3 shows a photograph of the ESD twin screen color graphics terminals with the laser screen as the control panel. Figure 4 shows the main hardware components. (Millheim, 1983) aim was to build a drilling simulator where all drilling mechanisms could be interactive such that an engineer could virtually drill a well with the computer either in real time or faster than real time. The ESD was designed to generate any subset from an internal previously developed data base and originate a complete drilling system with a step-by-step procedure where the ESD operator has the option to build each complete subset from scratch, redesign part of the subset, or choose a complete existing subset.

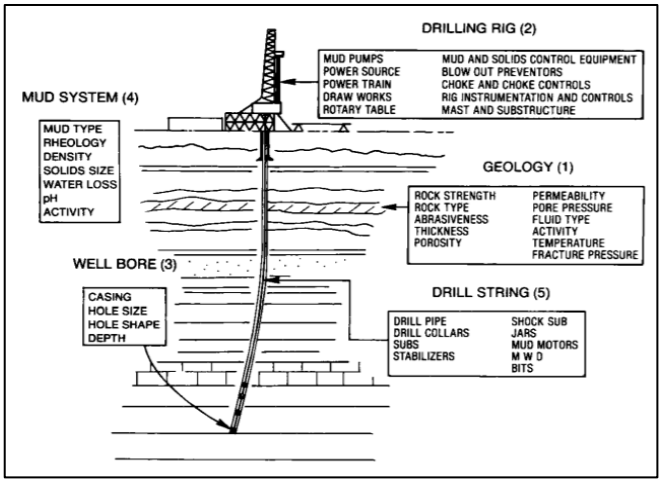

Figure 2: The Drilling System (Millheim, 1983)

Figure 3: Picture of the ESD (Millheim, 1983)

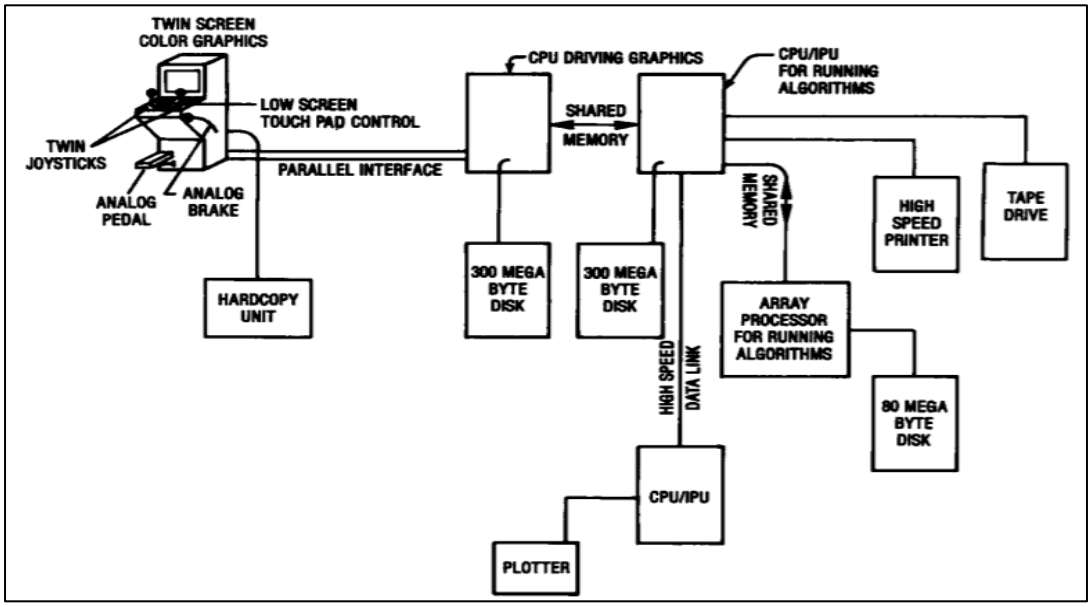

Figure 4: ESD Hardware Configuration (Millheim, 1983)

The ESD was created to drill depths of up to 30,000 ft where the geology can be subdivided into 2,000 elements with thicknesses ranging from 1 to 50 ft (Millheim, 1983). A geological drilling log (GDL) can be developed from the control well drilling data or inferred for an exploration well. It is important to obtain accurate drilling data for the ESD to approximate closer to actual drilling conditions. The ESD has a special GDL program that incorporates drilling and wireline logging data and allows the engineer to develop the drilling log as shown in Figure 5.

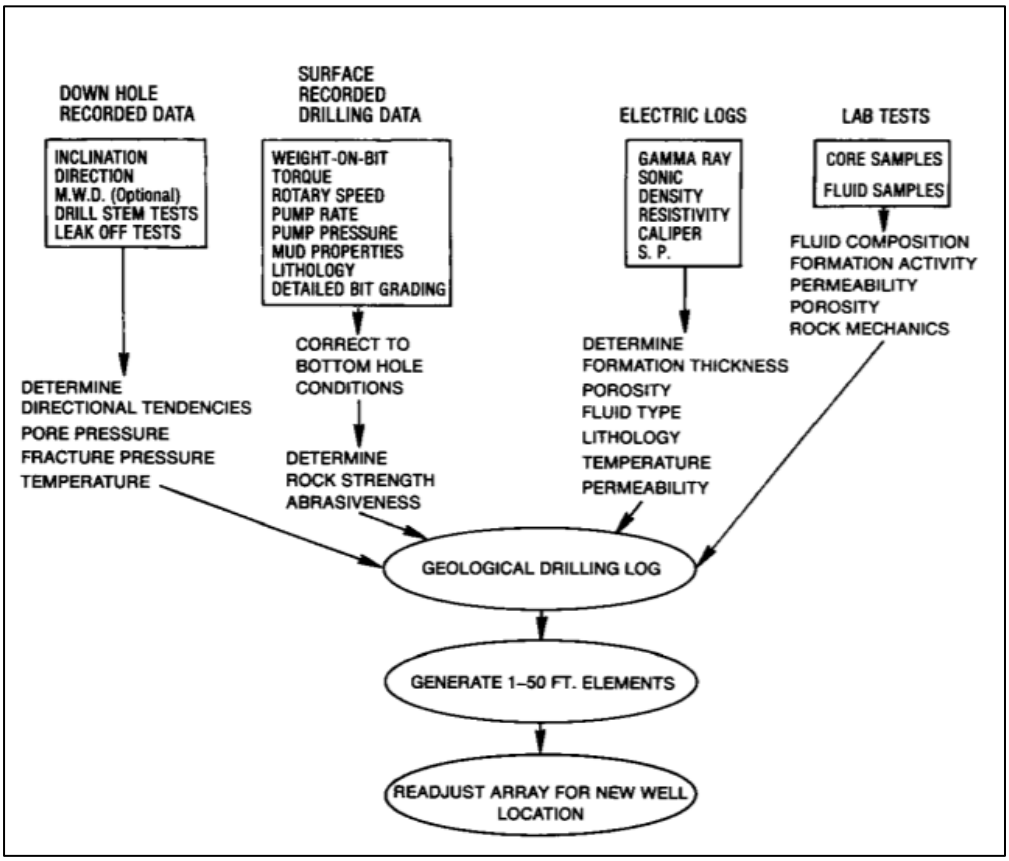

Figure 5: Development of Geological Drilling Log (GDL) (Millheim, 1983)

2.3.2 Geological Drilling Log Software (GDL) and Pason Drilling Simulator (PDS)

In 1994, Rampersad, et al. presented the Geological Drilling Log software which utilizes information obtained from a drilled well to optimize drilling costs for upcoming wells in the same field. The PDS software was built around a drilling-mechanics model that predicts the rate of penetration and rate of wear of a drill bit as a function of the type of bit, the rock being drilled, and the set of operational parameters, as presented by Bratli et al. (1997). The GDL and PDS software both use inverted ROP drilling models specific to the bits used for individual intervals to generate a formation profile of properties for the entire section drilled on a foot by foot basis (Rampersad et al., 1994). The GDL software was not only created to improve the current understanding of the effects of drilling parameters, but also present methods to effectively optimize the drilling process.

The drilling models used in both software are capable of reproducing realistic ROPs and accurately simulating an oil well.

The GDL software accounts for the effect of the geological environment in determining optimum drilling, which had never been introduced before in drilling simulation technology. Information extracted from a drilled well in a field is used to create a GDL, as shown in Figure 6. The GDL software contains rock strength with an example outlook depicted in Figure 7, which is incorporated into the drilling models under specified conditions to calculate ROP on a foot-by-foot basis. Through a series of simulation runs, optimum operating conditions for the lowest cost can be generated.

The Pason Drilling Simulator (PDS), was developed based on the Geological Drilling Log (GDL) and data collected from a previous well drilled in the same area and has been proven to reduce drilling costs by more than 50% (Gjelstad et al., 1998). The performance of different drilling parameters is evaluated through a series of simulations to create an optimum drilling program for a new well to be drilled. Just like the GDL, the simulator itself contains an algorithm that determines the ROP and rate of wear of the bit as drilling proceeds (Bratli et al., 1997).

The PDS also allows the user to change hydraulic programs, bit types, weight-on-bit (WOB), rotation per minute (RPM), detailed bit parameters and designs, time and cost per meter or foot calculation, section split or merge while considering bit wear during drilling (Mofrad, 2005). Evaluation of different options is made easy by using the artificial intelligence (AI) option that is built into the program. AI considers the ARSL to obtain results for a hard or soft formation (Mofrad, 2005).

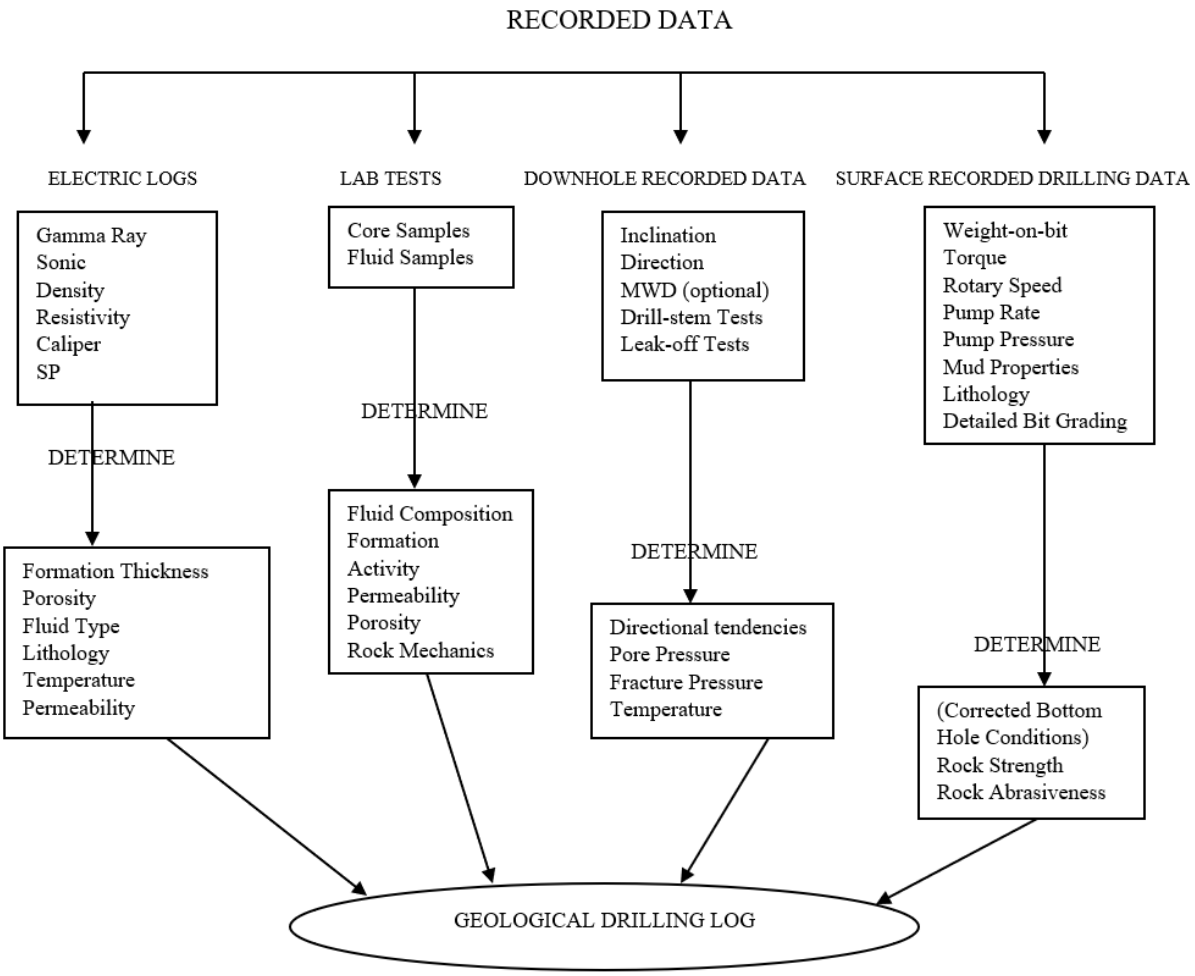

Figure 6: Creation of a Geological Drilling Log (Rampersad et al., 1994)

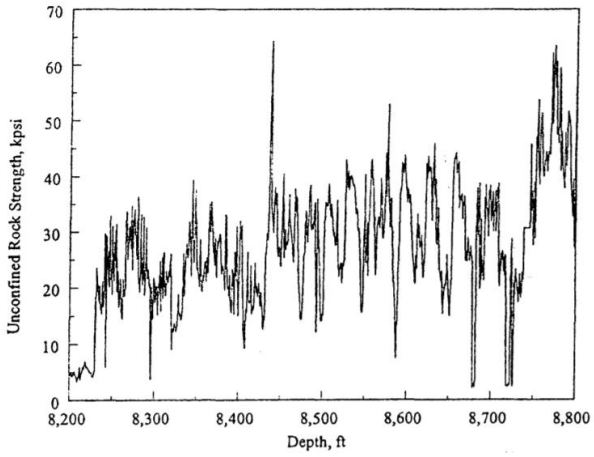

Figure 7: Unconfined Rock Strength Derived from the Inversion of Drilling Model (Rampersad et al., 1994)

2.3.2.1 ROP models

Hareland and Nygaard (2007) studied the importance of optimizing ROP for efficient drilling and created ROP models to calculate ARS. Drilling optimization by utilizing ROP models has reduced drilling costs substantially (Hareland and Nygaard, 2007). ROP models are mathematical models which describe how the penetration rate is affected due to changes in operational drilling parameters, changes in the rock properties and changes in bit types and design (Hareland and Nygaard, 2007). Several operational drilling parameters influence the ROP and are therefore included in the model. An ROP needs to include the effect of all the parameters such as WOB, RPM, flow rate, mud density and viscosity. The rock properties of the formations penetrated will also affect the ROP. For example, the high abrasiveness of the rock will contribute to accelerated bit wear, which in turn reduces ROP. Drilling data, bit parameters, drilling conditions and a known ROP all provide data that is used in an ROP model to generate a drill ability resistance. The drillability resistance is the resistance the bit has to overcome in order to shear the rock (Hareland and Nygaard, 2007). The drillability resistance for different drilling parameters, bit designs and geologies can be developed where the goal is to create a unique rock strength log based on ROP models regardless of bit type or design (Hareland and Nygaard, 2007).

Kerkar et al (2014) presented a method for estimating rock properties and in-situ rock mechanical properties in every well, based on calibration from initial rock core analyses and routinely acquired drilling data. Kerker analyzed wells drilled in the Lower Triassic Montney Formation E Lobe, Alberta, Canada in order to predict rock strength from the depth and time-based drilling data. Well A was used for the case study and the well's orientation and geological layers encountered during the drilling operation are shown in Figure 8.

Era	Period	Formation Top	MD (m)
Mesozoic	Lower Cretaceous	Paddy	766.14
		Cadotte	793.22
		Harmon	835.89
		Notikewin	891.9
		Falher	952.65
		Wilrich	1171.42
		Bluesky	1237.51
		Gething	1267.49
		Cadomin	1420.55
	Jurassic	Nikanassin	1445.87
		Fernie	1616.11
		Nordegg	1721.52
	Triassic	Baldonnel	1751.1
		Pardonet	1740.35
		Charlie Lake Fm	1794.58
		Artex	2151.19
		Halfway	2162
		Doig	2211
		Phosphate (Upper)	2332
		Phosphate (Middle)	2346.38
		Phosphate (Lower)	2377.6
		Montney	2392.19
		MNTN E Lobe	2396.32

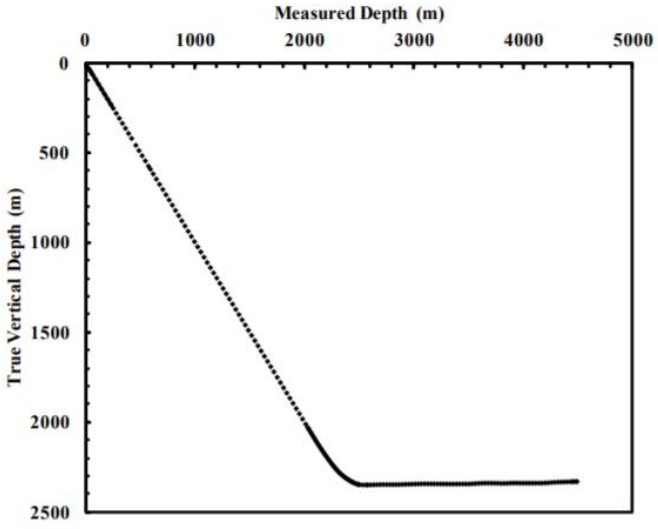

Figure 8: Formation Intervals and plot of true vertical depth against measured depth for the horizontal well (Well A) completed in Montney Formation E lobe

The depth-based data used in this case study were in 0.5m (1.6ft) increments, while the time-based data were every 20s. Figure 9 shows the drilling parameters used as inputs into the D-Series software along with the survey data. Table 5 shows the pore pressure, mud weight, plastic viscosity and mud type which were extracted from daily drilling reports. The pore pressure of the well measured as 14.58 kPa/m at a specific gravity of 1.49 which confirmed underbalanced drilling in the lateral section (Kerkar et al., 2014). Drill string specifications were also obtained from daily drilling reports and are listed in Table 6. An MSF513M PDC bit from Reed Hycalog was used to drill the horizontal section of the well. The bit specifications are listed in Table 7. Additional drilling parameters consisting of weight of the hook, number of lines and sheave efficiency were set to 27 klbs, 10 and 98% respectively. The SWOB, hook load and topdrive RPM of the well where the measured hook load was adjusted for frictional losses in the sheaves of the hoisting system are displayed in Figure 10. This adjustment was done after subtracting the weight of the block. The

effect of the sheaves on the hook load is displayed in Equations 1 and 2, where Equation 1 refers to the raising block and Equation 2 is the lowering block.

$$SheaveHL = \frac{HL_{obs}}{n_{lines}} \cdot \frac{e \cdot (1 - \frac{1}{e^{n_{lines}}})}{e-1} \qquad \textit{Equation 1}$$

$$SheaveHL = \frac{HL_{obs}}{n_{lines}} \cdot \frac{1 - e^{n_{lines}}}{1-e} \qquad \textit{Equation 2}$$

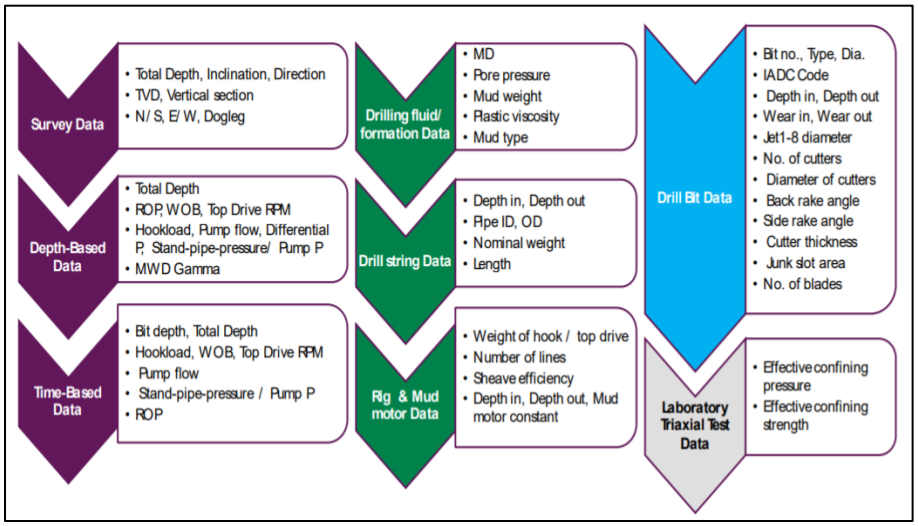

Figure 9: Summary of inputs used in DWOB-DROCK software calculations

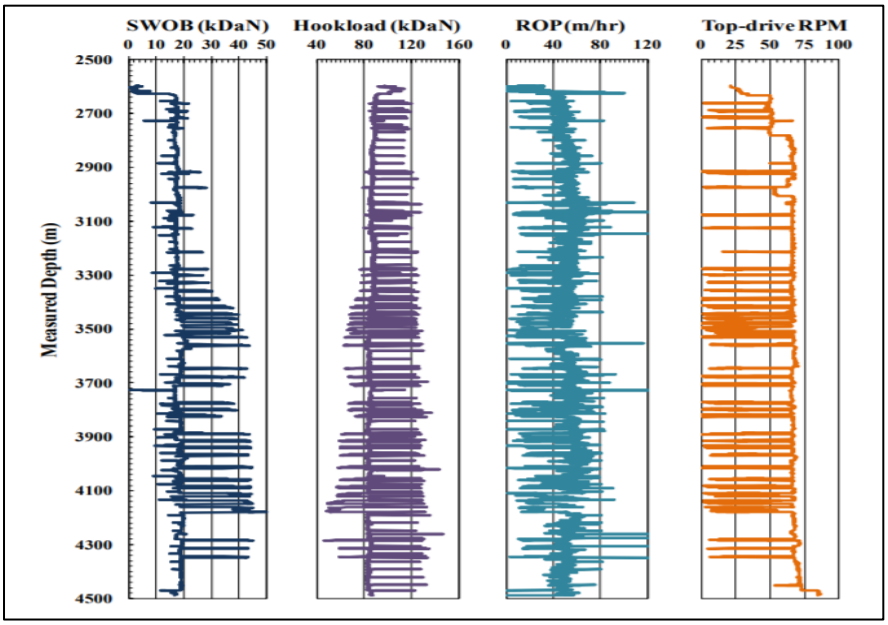

Figure 10: SWOB, HL, ROP and top-drive RPM from depth-based file of Well A

Table 5: Depth resolved pore pressure, drilling fluid characteristics of Well A

Depth m	Pore Pressure kPa/m	Mud weight g/cc	Plastic viscosity mPa-s	Mud Type
2740	14.58	1.04	21	Oil-based
3504	14.58	1.03	19	Oil-based
4237	14.58	1.005	12	Oil-based
4490	14.58	1.355	30	Water-based

Table 6: Drill string specifications at total depth of well A

Component Type	Joints	Length m	OD mm	ID mm	Specific mass Kg/m
Drill Pipe	192	1836.34	163	108	32
HWDP	39	362.91	164	77	70
Drill pipe	233	2250.35	163	71	32
Crossover	1	0.91	167	71	148
Flexible Drill Collar	1	8.79	155	73	148
Flexible Drill Collar	3	9.23	165	73	148
Pulser sub	1	2.93	149	59	148
MWD Tool	1	5.76	159	83	148
Crossover	1	0.65	157	78	148
Non-mag Pony Collar	1	2.99	166	73	148
Bent Housing	1	8.87	184	0	148
PDC	1	0.27	200	0	148
Total Length		4490			

Table 7: Design specifications of Reed Hycalog MSF513M PDC drill bit

IADC Code	513
Diameter (mm)	200
Number of nozzles	7
Diameter of each nozzle (mm)	11.1
Number of cutters	33
Diameter of cutter (mm)	12.7
Back rake angle (deg.)	20
Side rake angle (deg.)	0
Cutter thicknerss (mm)	2
Junk slot area (mm^2)	76
Number of blades	5

The resultant hook load was then further corrected by subtracting the product of the differential pressure and cross sectional area of the drill pipe. The weight of each element of the drillstring was calculated from the drill string weight of that element multiplied by the buoyancy factor (Kerkar et al., 2014). In order to determine if the element was in tension or compression, ((Kerkar et al., 2014) used the survey data as a reference. The forces were then added up from the bottom to the surface in an effort to compute the net hook load. Time-based data was used to identify off-bottom calibration depths at which friction factors were determined iteratively to match the surface hook load and net hook load within a 0.5 kDaN tolerance using Equations 3 and 4. The DWOB was adjusted by applying standpipe pressure correction to the hook load. DWOB values could be further subjected to potential sliding criterion shown in Equation 5 in the buildup section of the wellbore and abrasiveness for different formations are shown in Table 8.

$$F_{top} = \beta w \Delta L \left(cos\alpha \ or \ \frac{sin\alpha_{top} - sin\alpha_{bottom}}{\alpha_{top} - \alpha_{bottom}} \right) - \mu \times \beta w \Delta L \left(sin\alpha \ or \ \frac{cos\alpha_{top} - cos\alpha_{bottom}}{\alpha_{top} - \alpha_{bottom}} \right) + (F_{bottom} - DWOB \ or \ [F_{bottom} - DWOB] \times e^{-\mu|\theta|}) \quad \textit{(no bending)} \qquad \textit{Equation 3}$$

$$F_{top} = \beta w \Delta L \left(cos\alpha \ or \ \frac{sin\alpha_{top} - sin\alpha_{bottom}}{\alpha_{top} - \alpha_{bottom}} \right) - \mu \times \beta w \Delta L \left(sin\alpha \ or \ \frac{cos\alpha_{top} - cos\alpha_{bottom}}{\alpha_{top} - \alpha_{bottom}} \right) + (F_{bottom} \ or \ F_{bottom} \times e^{-\mu|\theta|}) \quad \textit{(bending)} \qquad \textit{Equation 4}$$

If RPM > 14, no correction in WOB where, $constant = \frac{(\frac{WOB}{\Delta P})_{i-2} + (\frac{WOB}{\Delta P})_{I-3} + (\frac{WOB}{\Delta P})_{i-4}}{3}$

If RPM < 14, $WOB_{slide} = constant \times \Delta p$ *Equation 5*

Table 8: Typical gamma ray and abrasiveness constants for different rock types

Formation	Specific gravity -	Abrasivess constant -	Gamma ray API
Sand	2.6	1	10-30
Silts	2.67-2.7	0.85	50-70
Conglomite	2.4-2.9	0.71	10-140
Dolomite	2.7	0.65	<30
Limestone	2.7	0.57	<20
Shale	2.4-2.8	0.11	80-300
Coal bituminous	1.35	0.1	20

After selecting a percentage value for SWOB as DWOB, the ROP model developed for PDC drill bits presented by (Hareland and Nygaard, 2007) as illustrated by Equation 6 was used. The PDC ROP model considers a force balance between one cutter and the formation in order to derive an analytical solution for the entire drill bit face with multiple cutters. The model was empirically calibrated with laboratory data obtained with prototype bits tested on a variety of formations. The empirical relation was further corrected for drill bit wear function as displayed by Equations 7 and 8 depending on formation abrasiveness and wellbore cleaning efficiency based on hydraulics. Equations accounting for hydraulics are displayed by Equations 9 and 10. In addition to bit wear and hydraulic efficiency, the number of blades of a PDC is considered to lower the drilling efficiency, this effect is applied using Equation 11. (Kerkar et al., 2014), iteratively matched the calculated ROP to the measured ROP to calculate CCS. The coefficients a_2, b_2 and c_2 were determined from laboratory tests performed under simulated borehole conditions. The CCS can then be correlated to the UCS by using regression constants obtained from laboratory triaxial tests. Equations correlating the CCS to the UCS are presented by Equations 12.

$$ROP = \left[\frac{K_1 \cdot WOB^{a_1} \cdot RPM^{b_1} \cdot cos(SR)}{CCS^{c_1} \cdot D_b \cdot tan(BR)}\right] \cdot W_f \cdot h(x) \cdot b(x) \qquad \textit{Equation 6}$$

$$W_f = 1 - a_3 \left(\frac{\Delta BG}{8}\right)^{b_3} \qquad \textit{Equation 7}$$

$$\Delta BG = Ca \sum_{i=2}^{n} WOB_i \cdot RPM_i \cdot CCS_i \cdot ABR_i \qquad \textit{Equation 8}$$

$$h(x) = a_2 \cdot \frac{\left(HSI \cdot \frac{JSA}{2 \cdot D_B}\right)^{b_2}}{ROP^{c_2}} \qquad \textit{Equation 9}$$

$$HSI = \frac{HHP}{A_B} = \frac{[Q \cdot P_B / 1714]}{[(\frac{\pi}{4}) \cdot D_B^2]} \qquad \textit{Equation 10}$$

$$b(x) = \frac{RPM^{(1.02 - N_b x 0.02)}}{RPM^{0.92}} \qquad \textit{Equation 11}$$

$$UCS = \frac{CCS}{1 + a_s \cdot Pc^{b_s}} \qquad \textit{Equation 12}$$

ROP models calculate the rock strength at the bit operating conditions at bottom hole. In ordinary drilling parameters, the mud weight is higher than the conditions, therefore ROP models only calculate the confined rock strength. Unconfined rock strength can be found using equation 12 Figure 11 shows sample values for a_s and b_s constants which are calculated based on triaxial testing.

$$S = S_o(1 + a_s \cdot pe^{b_s}) \qquad \textit{Equation 13}$$

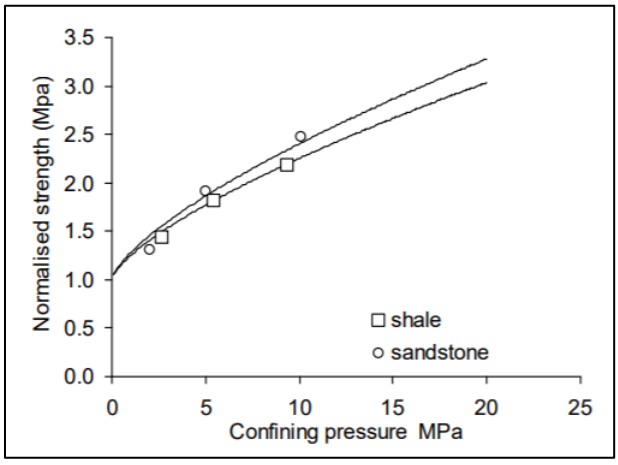

Figure 11: Determination of a_s and b_s values for shales and sandstones (Hareland and Nygaard, 2007)

2.3.2.1.1 ROP Model for Roller/Tricone Bits

Hareland and Nygaard (2007) published the ROP models for the two main bit designs that are used in the drilling industry. An example of a tricone bit is shown in Figure 12. The two main bit designs used are roller cone and drag bits. Roller cone bits have three cones which rotate around their axis while drag bits consist of a fixed cutter mechanism which can include cutter blades, diamond stones or cutters. The most common type of drag bits are PDC bits which make use of Polycrystalline Diamond Compact (PDC) cutters mounted on the bit's blades or body. The drag bits work by fracturing the rock through shearing. Because of the differences in bit design and different fracturing abilities observed, the different bit types are treated separately in the ROP models. Equation 14 shows the ROP model for roller cone bits as proposed by Warren (1984).

$$ROP = \left(\frac{aS^2 d_b^3}{RPM^b WOB^2} + \frac{b}{RPM d_b} + \frac{c d_b^3 \mu MW}{0.000516 \rho q v_n}\right)^{-1} \qquad \textit{Equation 14}$$

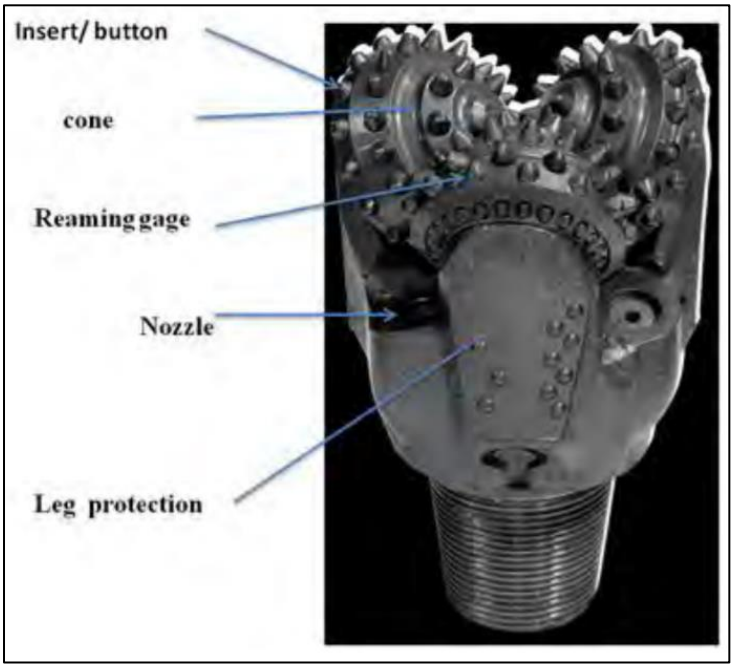

Figure 12: Tricone bit example (Barzegar et al., 2014)

The first term of equation 14 defines the maximum rate at which the rock is broken into small chips by the bit, the second term modifies the predictions to account for the distribution of the applied WOB to more teeth as the WOB is increased and the teeth penetrate deeper into the rock, and the

third term models the rate at which the cuttings are removed from the bottom based on the hydraulic impact force and the properties of the mud for one set of nozzles (Warren, 1984).

The Warren model excludes two important parameters which also alter the ROP. The Warren model does not consider the effect of overbalance created by the pressure difference (pe) between mud weight (MW) and pore pressure (PP). This effect is outlined in equation 15.

$$pe = MW - PP \qquad \textit{Equation 15}$$

Hareland and Hoberock (1993) describe a phenomenon called the chip hold effect that occurs when the higher mud weight, compared to the pressure in the pores below the bit, pushes the already drilled rock chips to the bottom, thus reducing the effectiveness of the cleaning. Hareland and Hoberock (1993) accounted for this effect by including the following term in the Warren (1984) ROP model:

$$fc(pe) = cc + ac(pe - 120)^{bc} \qquad \textit{Equation 16}$$

The second effect that is not accounted for in this model is bit wear. When roller cone bits start to wear and become dull, the stress on each cutter is reduced and the dullness increases, thus reducing ROP. To account for bit wear, Hareland and Nygaard (2007) introduced the effect of bit wear in the ROP model as given in equation 17 below.

$$Wf = 1.0 - \frac{Wc \sum_{i=1} WOB_I RPM_I Abr_i S_i}{8.0} \qquad \textit{Equation 17}$$

Including the bit wear in the ROP model yields a new ROP equation, which is given in equation 18.

$$ROP = Wf \left(fc(pe) \left(\frac{aS^2 d_b^3}{RPM^b WOB^2} + \frac{b}{RPM d_b} \right) + \frac{c d_b^3 \gamma f \mu}{0.0005516 \rho q v_n} \right)^{-1} \qquad \textit{Equation 18}$$

Equation 18 models the effects that different operating conditions and rock strength have on ROP. The rock strength calculated using this model does not give a uniform rock strength that is universally transferrable from well to well when bit design is changed. Therefore, a large number

of field and laboratory observations have been analyzed to observe the effect of various operational parameters on ROP for rollercone bits. Figure 13 shows the results that were observed from the analysis. Figure 13 depicts different operational condition effects on ROP for a rollercone bit. To accommodate the results from figure 13, the ROP equation is modified to better simulate the operational effects on ROP to the form expressed as equation 19.

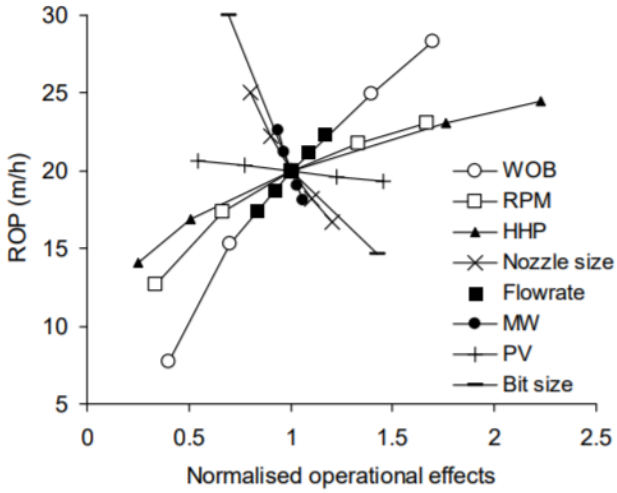

Figure 13: Normalized effects of operational parameters on ROP for rollercone bits. HHP is hydraulic horsepower. PV is plastic viscosity (Hareland and Nygaard, 2007)

$$ROP = Wf\left(f(hyd)\left(\frac{aS^{2-bs}d_b^2}{RPM \cdot WOB^{2-bs}}\right)\right)^{-1} \qquad \textit{Equation 19}$$

The chip hold function and cutter cleaning of the ROP model in equation 16 is replaced by an effect based hydraulic formula that treats the effect of flow rate, mud weight and plastic viscosity, hydraulic horsepower, and nozzle sizes according to Figure 13. The rock strength can then be calculated by inverting the rollercone bit ROP model in equation 18.

2.3.2.1.2 ROP Model for PDC bits

PDC bits have different design parameters than rollercone bits and fail the rock by shearing. ROP models for PDC bits must therefore treat bit designs differently than rollercone ROP models. Figure

14 shows an example of a PDC bit. The operational effects on a set ROP of 30 m/hr for PDC bits are shown in Figure 15 and the bit design parameters are shown in Figure 16. The various operational parameters have similar ROP trends for both PDC and rollercone bits. Therefore, it can be expected that the ROP model for PDC bits can be of a similar form as the ROP model for rollercone bits. The ROP model for PDC bits as presented by Kerkler et al (2014) is given by Equation 6.

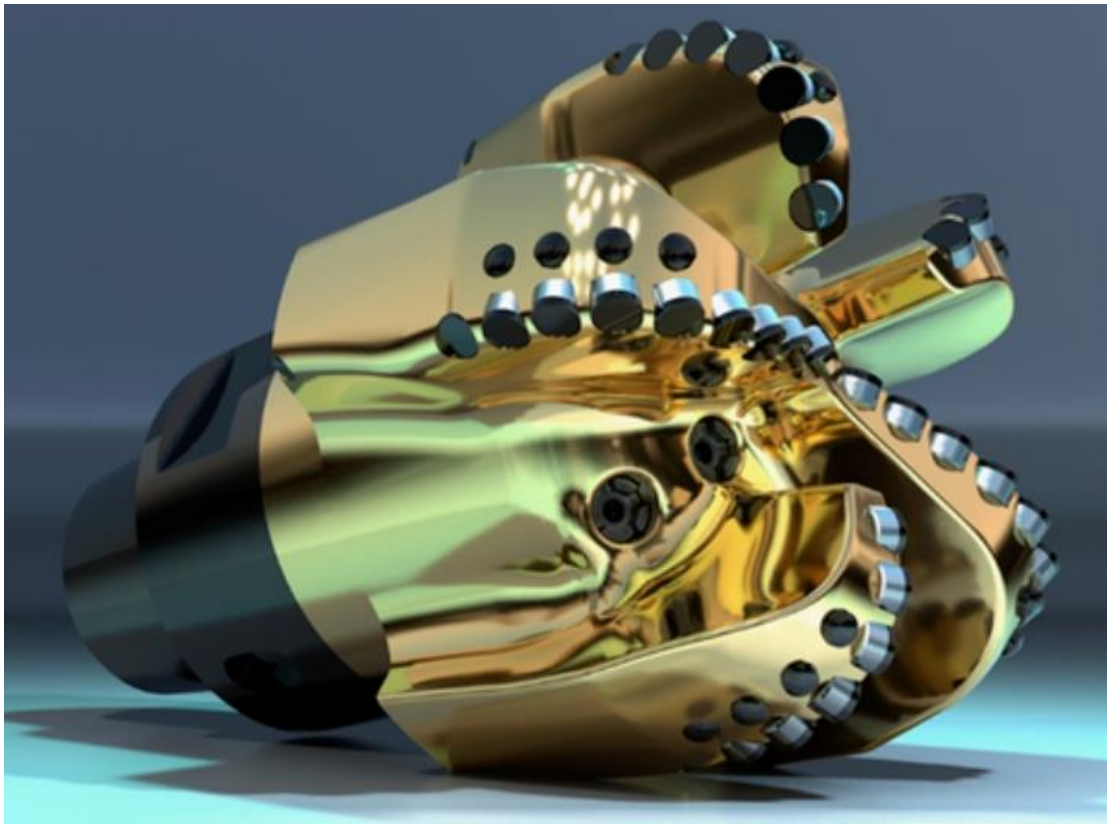

Figure 14: PDC bit (Image from Baker Hughes)

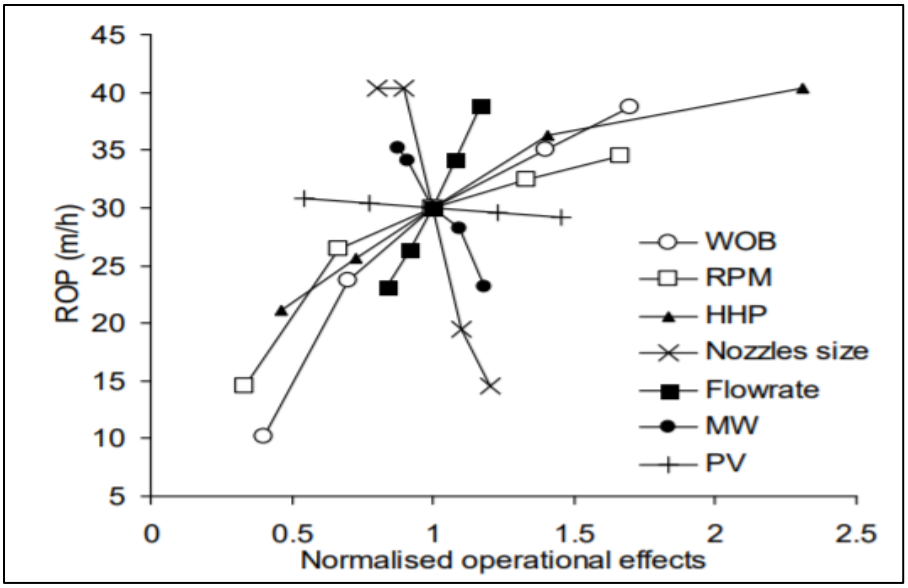

Figure 15: Normalized effects of operational parameters on ROP for a PDC bit (Hareland and Nygaard, 2007)

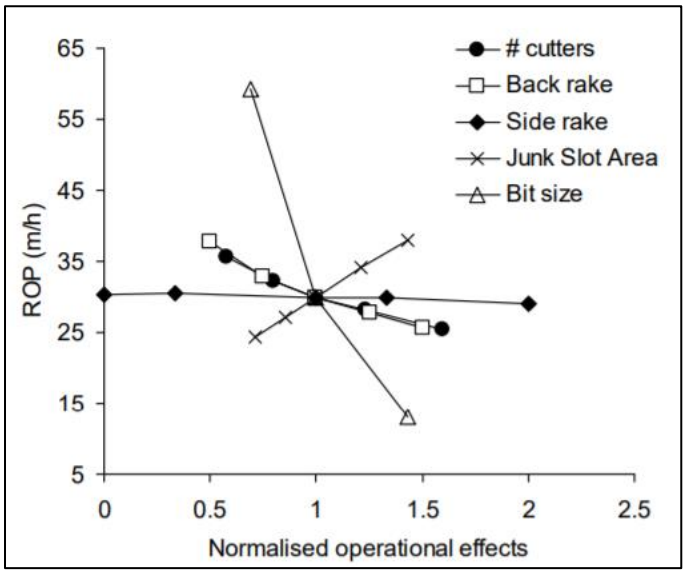

Figure 16: Normalized effects of PDC bit design parameters on ROP (Hareland and Nygaard, 2007)

2.3.2.1.3 Natural Diamond Bit Model

The Natural Diamond Bit (NDB) model was developed by Rampersad et al. (1994) to be used if a well is to be drilled with NDBs. The NDB model was designed to allow rock penetration by

applying a certain WOB on each diamond. The ROP model for NDBs is given by Equation 20. Figure 17 depicts an example of an NDB.

Figure 17: Natural Diamond bit (Al Dushaishi, Fall 2020)

$$ROP = \frac{14.14 \cdot N_s \cdot RPM \cdot (A_v - A_{vw}) \cdot corr}{D_{bit}} \qquad \textit{Equation 20}$$

Equations 21 and 22 calculate the mechanical weight on bit where ΔP is the pump off force acting on the face of the bit. The equivalent bit radius is defined by Equation 23, and the volume worn by each cutter per bit revolution is given by Equation 24. Values for bit data are shown in Table 9.

$$WOB_{mech} = WOB_{applied} - \Delta p A_p \qquad \textit{Equation 21}$$

$$\Delta p = \frac{GPM^2 \rho}{12031(KA)^2} \qquad \textit{Equation 22}$$

$$R_e = \frac{D_{bit}}{2\sqrt{2}} \qquad \textit{Equation 23}$$

$$V_D = C_a \cdot \sum_{i=1}^{n} \frac{WOB_{mech} \cdot RPM_i \cdot S_i \cdot Ar_{abr_i}}{N_s \cdot R_e} \qquad \textit{Equation 24}$$

Table 9: Diamond Bits Data (Rampersad et al., 1994)

Bit No	Diamond Wear Coefficient	Cost ($)	No. of Stones	Diamond Diameter (in)	Pump-Off Area (in^2)
4	4.26×10^{-11}	28,000	823	0.133	5.26
5	4.26×10^{-11}	28,000	816	0.139	8.86
6	4.26×10^{-11}	28,000	1192	0.137	9.60
7	4.26×10^{-11}	28,000	3019	0.095	11.86

Equations 25 and 26 calculate the penetration of each diamond and penetration loss due to wear of diamond respectively. The front projected area of each diamond is calculated from Equation 27, while the projected area of the worn section of a diamond is calculated from Equation 28. Rampersad, et al. (1994) accounted for a lithology correction factor shown in Equation 29 which is applied to account for anomalies.

$$P = \frac{2}{\pi \cdot d_s}\left(\frac{WOB_{mech}}{S \cdot N_s} - \frac{\pi P_w d_s}{2}\right) \qquad \textit{Equation 25}$$

$$P_w = \sqrt{2} \cdot \frac{V_D}{\pi d_s} \qquad \textit{Equation 26}$$

$$Av = (\frac{d_s}{2})^2 \cdot cos^{-1}(1 - \frac{2P}{d_s}) - \sqrt{d_s \cdot P - P^2}(\frac{d_s}{2} - P) \qquad \textit{Equation 27}$$

$$Avw = (\frac{d_s}{2})^2 \cdot cos^{-1}(1 - \frac{2P_w}{d_s}) - \sqrt{d_s \cdot P_w - P_w{}^2}(\frac{d_s}{2} - P_w) \qquad \textit{Equation 28}$$

$$corr = a_d / RPM^{b_d} \cdot WOB^{c_d} \qquad \textit{Equation 29}$$

Using the GDL software together with the appropriate bit models calculates the ROP at any particular depth (Rampersad et al., 1994). The calculation for cost per foot is given by Equation 30

and the process for determining best cost is outlined in Figure 18. For this particular study, Rampersad, et al maintained the drilling pressure differential at a constant overbalance of 300 psi and the rig cost was set at $600/hr. The tripping and connection times were kept at 1hr/1000ft per round trip and 5 min/30ft respectively. Figure 19 shows a typical learning curve obtained from running 20 simulations, which proves that by running numerous simulations and adjusting drilling parameters, it is possible to obtain the lowest drilling cost (Rampersad et al., 1994).

$$C_f = \frac{(t_r+t_t+t_c)C_r+t_rC_m+C_b}{D} \qquad \textit{Equation 30}$$

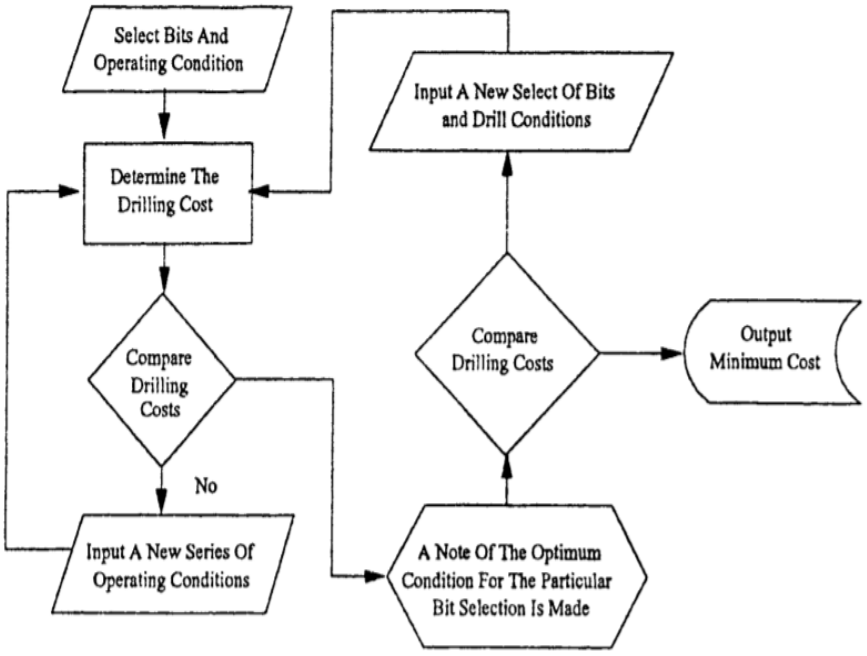

Figure 18: Steps in Obtaining Optimum Drilling Cost (Rampersad et al., 1994)

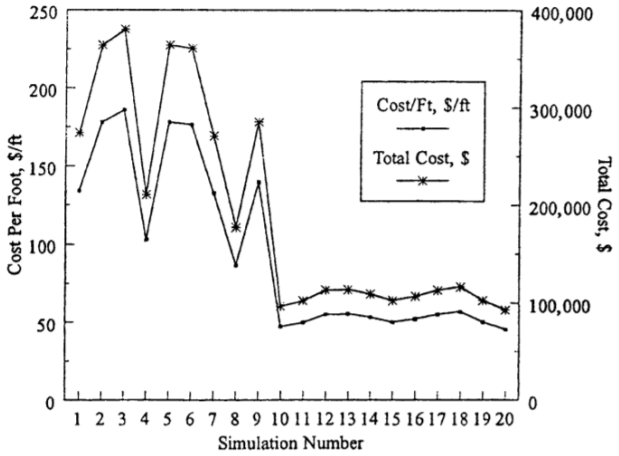

Figure 19: Learning Curve for the Interval Drilled (Rampersad et al., 1994)

2.3.3 Virtual Experience Simulation (VES)

Various drilling simulators have been developed to aid in drilling efficiency. In 1999, Millheim and Gaebler created the VES software to account for huge drilling data accumulations that evolve from wells drilled in the past. VES software provides a way to retain field drilling experience so that it can be easily accessed and learned by others. Based on a concept of heuristics, which creates an interactive learning experience for the user, the unused drilling data is activated into data sets for geology, cementing, tripping, logging, penetration rate and unscheduled events. According to Millheim and Gaebler (1999), these data sets are then able to retain the field drilling experience and knowledge. The concept of heuristics offers a way to retain knowledge and experience that is specific to a specific geological and geographical area. Recounting of this knowledge is what is done via the use of VES. Figure 20 represents a critical paradigm of heuristics which suggests a model of the simulation of human thought, artificial intelligence and heuristic problem solving. Figure 21 shows inert data accumulation operated on by a method to convert the unused data into retained knowledge and potential learning. Millheim and Gaebler (1999) created the VES software in an effort to make job specific drilling knowledge readily available on a platform for employees to learn and access.

The process of data activation includes generating tripping times as a function of total depth drilled. Millheim and Gaebler calculated the tripping rates of 18 drilled wells by collecting tripping data and sorting them in ascending order. Two scatter plots, one for tripping in and one for tripping out were then generated as shown in Figure 22. Based on the plots, a second order curve fitting polynomial calculation is performed for each data set. The fitting equation is given by Equation 31 where the resulting parameters are shown in Table 10.

$$TripRate = A + B_1 * Depth + B_2 * Depth^2 \qquad \textit{Equation 31}$$

Table 10: Trip Rate Parameters (Millheim and Gaebler, 1999)

Parameter for the Trip Rate Calculation			
	A	B_1	B_2
Trip In	-266.00	0.49	-2.87e-5
Trip Out	584.86	0.36	-2.28e-5

To extract ROP data, Millheim and Gaebler first digitalized the data according to the specific layers taken from master logs containing mud properties, ROP (given in minutes needed to drill 5ft), lithology, hydrocarbon gas content and a geological description. Millheim and Gaebler found the importance of the influence of WOB and RPM on drilling performance. By using a technique called Isomeric mapping, the user of the software is able to set their decisions and compare different effects. Based on the need to give the user the flexibility of choosing WOB and RPM, the idea of interpreting the ROP as heights in topographical maps was formulated (Millheim and Gaebler, 1999). A software program called Surfer V6.02 was used to generate the isomeric maps and the dimensional models. Using data from 12 drilled wells, (Millheim and Gaebler, 1999) Millheim and Gaebler built a topographic map for one layer (No.15), where the ROP values were interpreted as heights. The isometric map and a 3D model were generated using Surfer V6.02 software as shown in Figures 23 and 24 respectively. Regions with better performance are highlighted and ranked. The numerals 1, 2, 3, and 4 identify regions where the combination of ROP and WOB

shows the best performance. The same analysis or data activation process can be made for each activity and parameter of the drilling operation.

Based on the activated data sets, a complete model is developed where the user has an interactive environment to gain insights of a certain domain and test different scenarios. A purpose-built software called PowerSim Constructor 2.5D was used to develop the heuristics engine to enable the transfer of knowledge stored in the activated data sets. The major data sets support five basic processes encountered during drilling which are actual drilling, setting casing, setting lost circulation plugs, logging, and coring. These processes are shown in Figure 25. The user's inputs are marked as shaded boxes and the probabilistically based heuristics are unshaded.

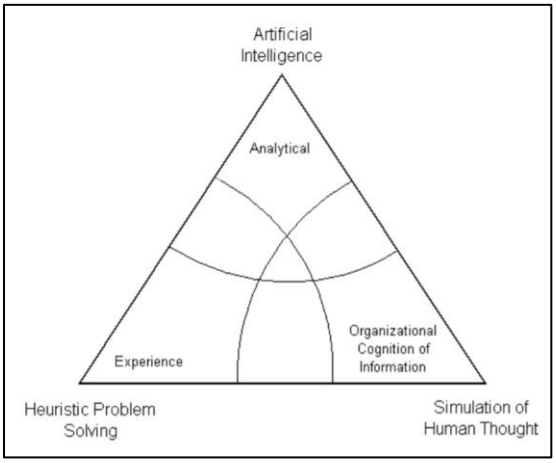

Figure 20: Heuristic Triangle (Millheim and Gaebler, 1999)

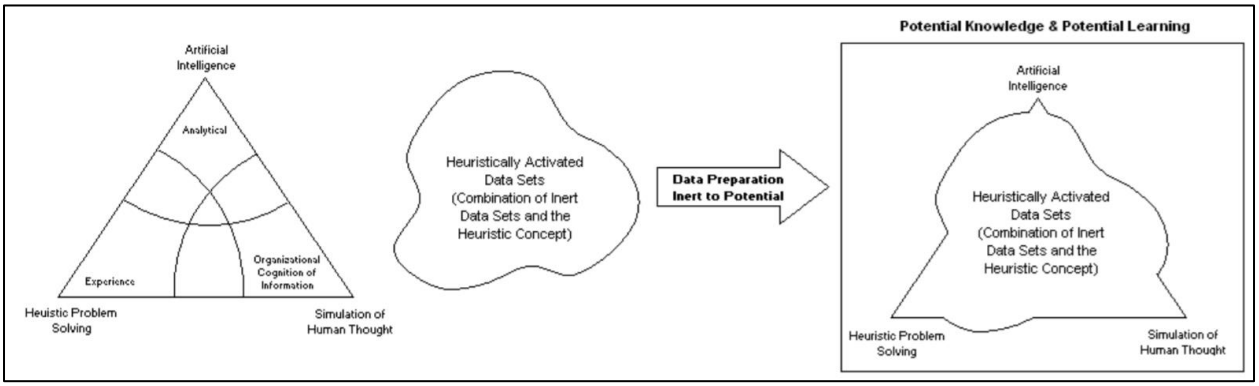

Figure 21: Merging Inert Data Set with the Heuristic Triangle (Millheim and Gaebler, 1999)

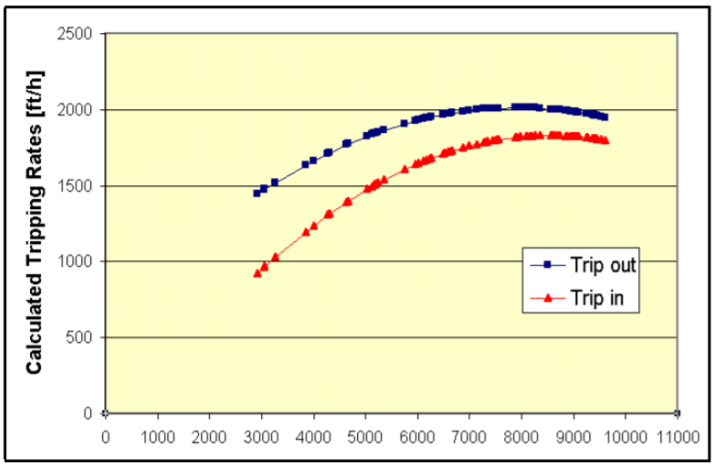

Figure 22: Trip Rate Derived from Actual Well Data (Millheim and Gaebler, 1999)

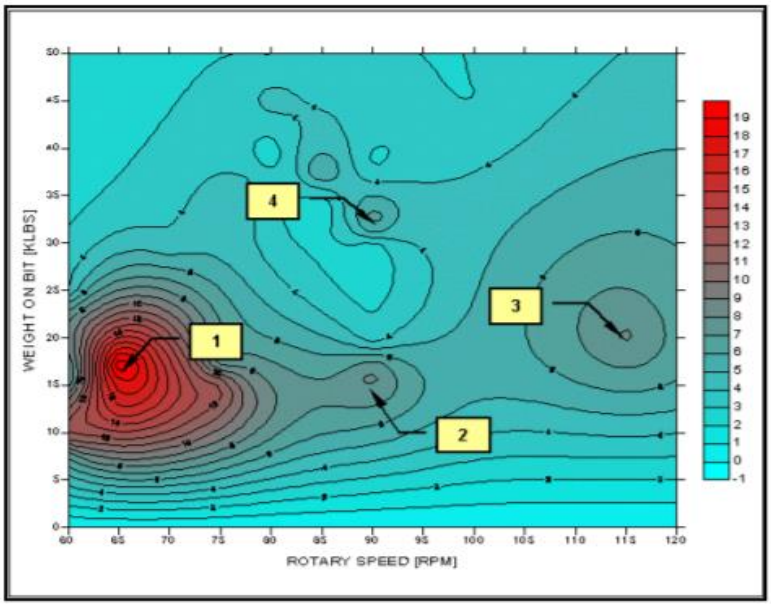

Figure 23: ROP Surface Map for Layer 15 in m/hr (Millheim and Gaebler, 1999)

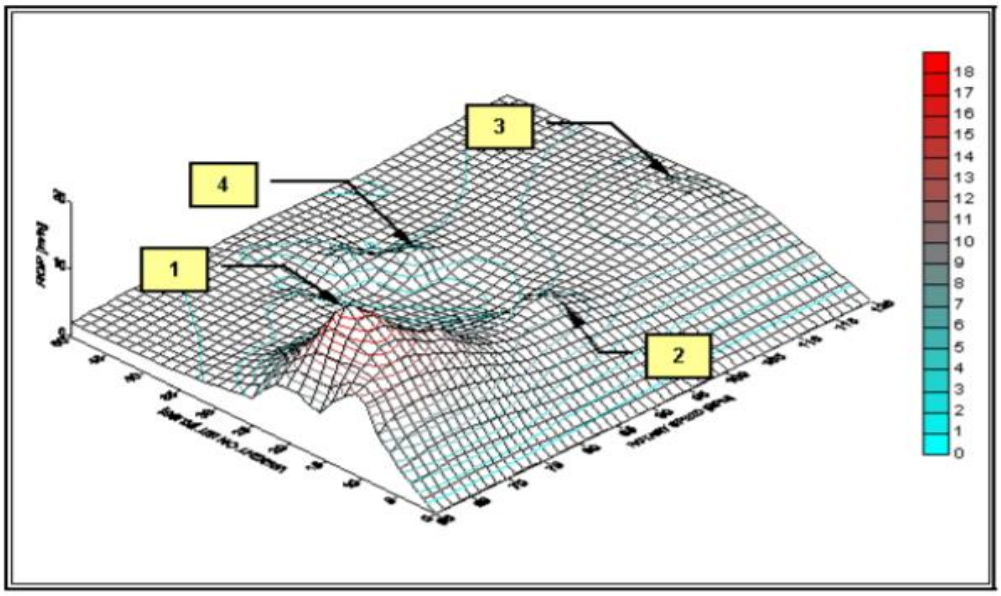

Figure 24: 3-Dimensional Surface Map of Layer 15 (Millheim and Gaebler, 1999)

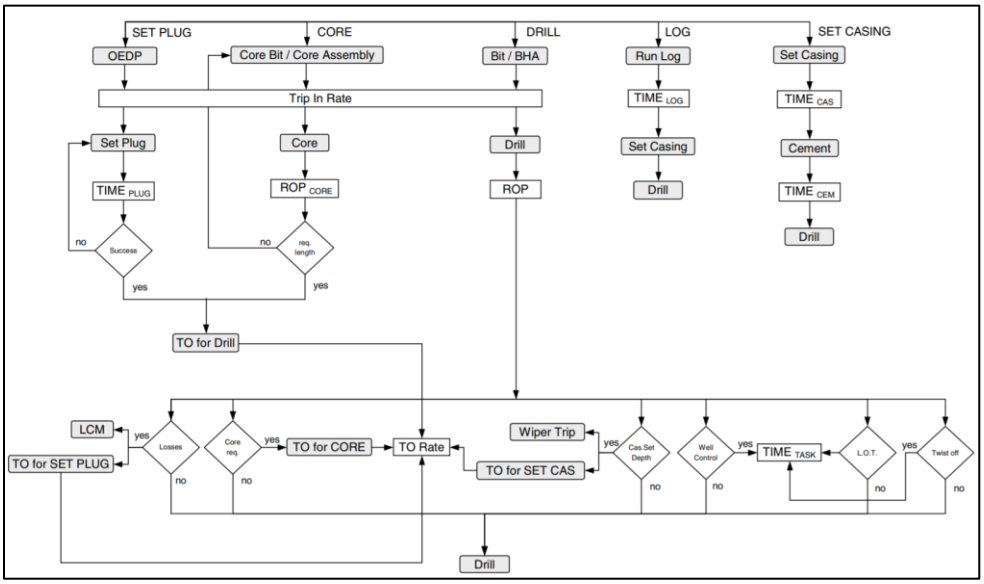

Figure 25: VESD Flow Diagram (Millheim and Gaebler, 1999)

2.4 Friction along the wellbore

Wellbore friction occurs between the drillstring and wellbore and can cause surface measurements of weight on bit and torque to differ significantly from downhole measurements. In 1987 Falconer, et al. presented a technique to determine friction losses in the drillstring on a foot-by-foot basis at

the wellsite by using a mathematical model based on trajectory of the wellbore and the weight and dimensions of the individual drillstring components. The model is based on the one proposed by Johncsik,et al. (1984) for determining side forces, tension, and torque losses for a drillstring in a given wellbore. The forces acting on an element of drillstring are the tensions at each end of the element and the buoyant weight of the element as shown in Figure 26. A friction factor for an element of drillstring can be calculated by Equations 32 and 33 if the torque and weight loss over the element are known. Friction forces acting on a drillstring are depicted in Figure 27 (Johancsik et al., 1984). Usually, the torque and weight losses at each element of the drillstring are not known, since only two measuring points are available that are at the drillfloor and at the mud tool. The model then uses the weight and torque losses calculated from the measurements of surface weight on bit (SWOB), MWD downhole weight-on-bit, surface torque, and MWD downhole torque. The outputs of DRAG (drillstring/wellbore sliding friction factor) and FRIC (drillstring/wellbore rotary friction factor) are the average friction factors along the whole drillstring from the MWD tool to the rotary table and can be calculated by Equations 34 and 35. DRAG usually ranges from 0.01 to 0.05, where anything above 0.05 indicates abnormal drilling while FRIC ranges from 0.15 to 0.13 are considered normal (Johancsik et al., 1984).

$$FRIC = \frac{torque\ loss\ over\ element}{element\ side\ force \times element\ radius} \qquad \textit{Equation 32}$$

$$DRAG = \frac{weight\ loss\ over\ element}{element\ side\ force} \qquad \textit{Equation 33}$$

$$FRIC = \frac{Torque\ loss\ over\ drillstring}{\sum_{MWD}^{Surface}[element\ side\ force \times element\ radius]} \qquad \textit{Equation 34}$$

$$DRAG = \frac{Weight\ loss\ over\ drillstring}{\sum_{MWD}^{Surface}[element\ side\ force]} \qquad \textit{Equation 35}$$

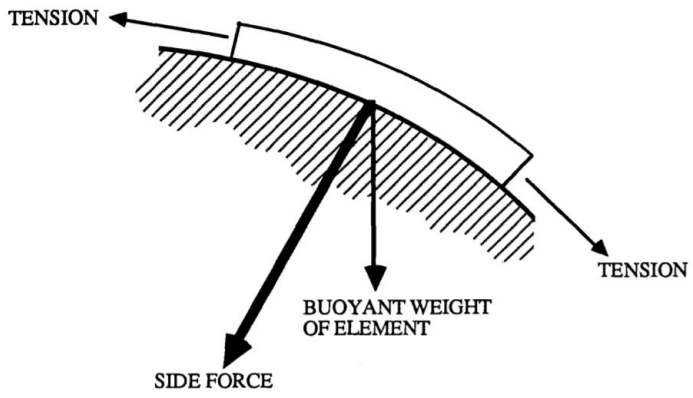

Figure 26: Forces acting on an element of drillstring (Johancsik et al., 1984)

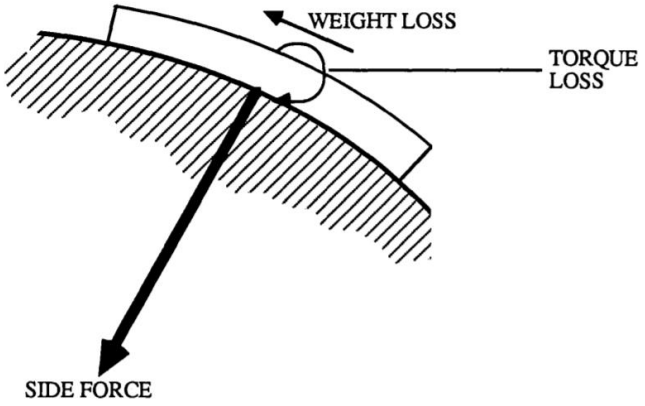

Figure 27: Friction forces acting on an element of drillstring (Johancsik et al., 1984)

In 2012, Wu and Hareland (2012) presented an application of the Finite Element Analysis (FEA) model which has the ability to simulate the working behavior of the drillstring during a drilling operation. The FEA model takes stiffness into consideration and can also be used to back-calculate the friction factor or coefficient between drillstring and casing or formation using off-bottom data. Two coordinate systems are required for the FEA of any complex wellbore or drillstring, as depicted in Figure 28. The working behavior of the system is then described by the following dynamic equations as displayed in Equation 36. Boundaries and constraints can also be applied regardless of the complexity of the wellbore as shown in Figure 29.

$$[M]\{\ddot{U}\} + \dot{[C]}\{U\} + [\dot{K}]\{U\} = \{F\} \qquad \textit{Equation 36}$$

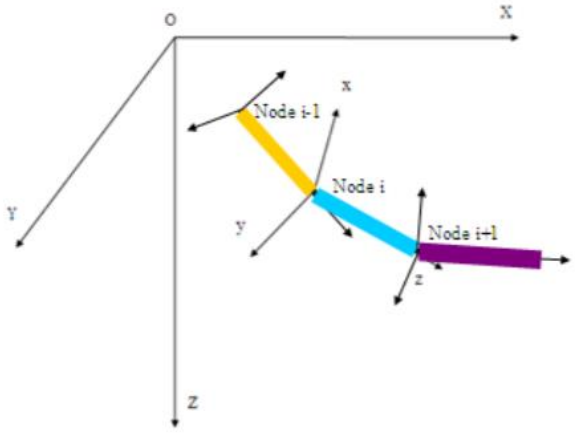

Figure 28: Discretization of the drillstring (Wu and Hareland, 2012)

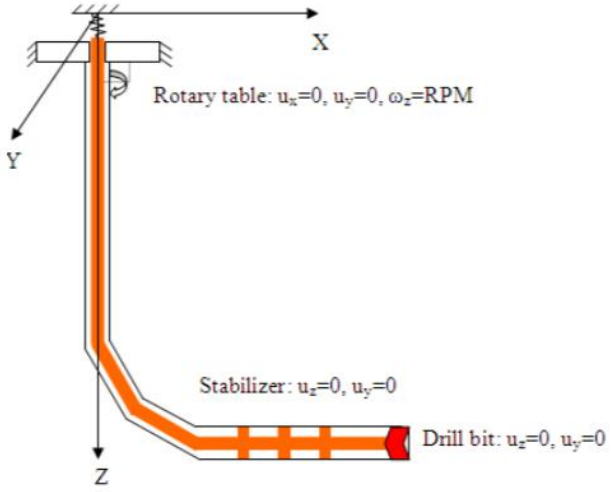

Figure 29: Boundary conditions applied (Wu and Hareland, 2012)

The normal force can be calculated by using equation 37 after the dynamic equations have been solved. The friction force can then be calculated using equation 38 if the friction coefficient is known (Wu and Hareland, 2012). Wu and Hareland (2012) calculated and analyzed the friction coefficients of two wells in western Canada (Well A) and the North Sea (Well B) using the FEA model. Well A measured over 14,763 ft in depth, while well B measured over 16,404 ft. Figure 30

shows well A's geometry along with the friction coefficients calculated at three different depths. Figures 31 and 32 show a comparison between the SWOB and DWOB as calculated by the FEA program for both well A and B respectively.

$$F_n = ((F_t \cdot \Delta\alpha \cdot sin\bar{\theta})^2 + (F_t \cdot \Delta\theta + W \cdot sin\bar{\theta})^2)^{\frac{1}{2}} \qquad \textit{Equation 37}$$

$$F_f = \mu \cdot F_n \qquad \textit{Equation 38}$$

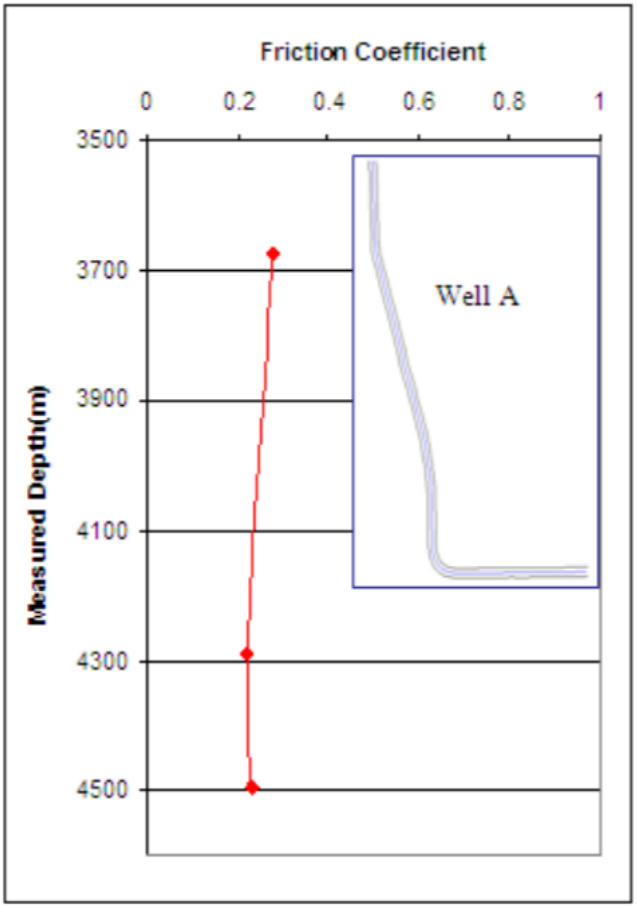

Figure 30: The coefficients from FEA (Well A) (Wu and Hareland, 2012)

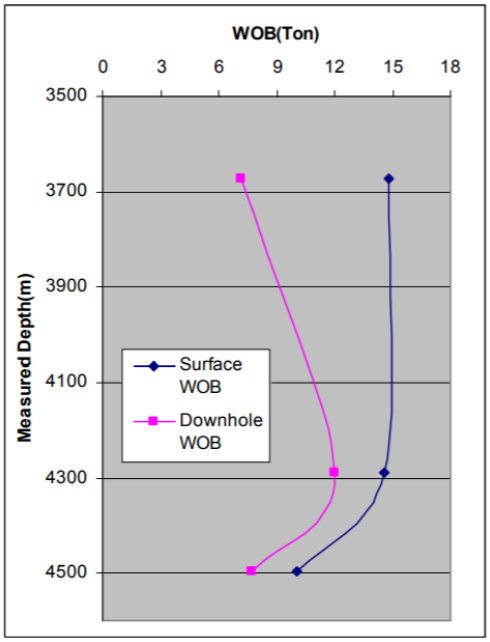

Figure 31: SWOB and DWOB from FEA (Well A) (Wu and Hareland, 2012)

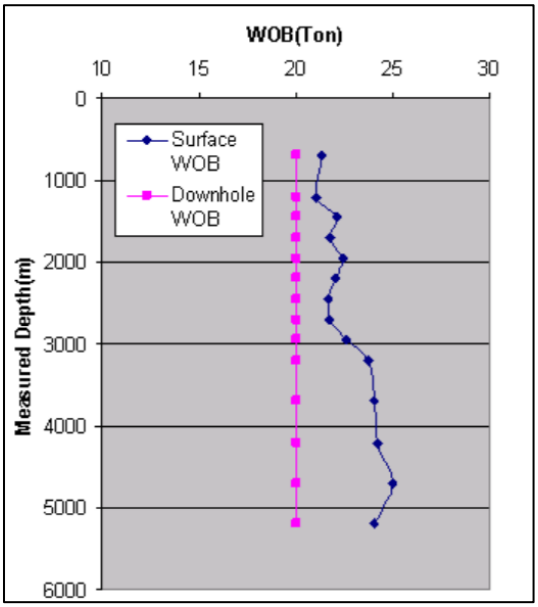

Figure 32: SWOB and DWOB from FEA (Well B) (Wu and Hareland, 2012)

2.5 D- Series Software

In 2017, Tahmeen et al. presented a cost-effective system composed of two D-Series software (D-WOB and D-Rock) developed to estimate wellbore friction coefficient, calculate down-hole

weight-on-bit and rock property logs from available surface drilling data. This method presents an effective and economic method for using typical drilling data to generate rock strength geomechanical logs without the extended costs of logging equipment. An overview of how the D-Series software works is shown in Figure 33.

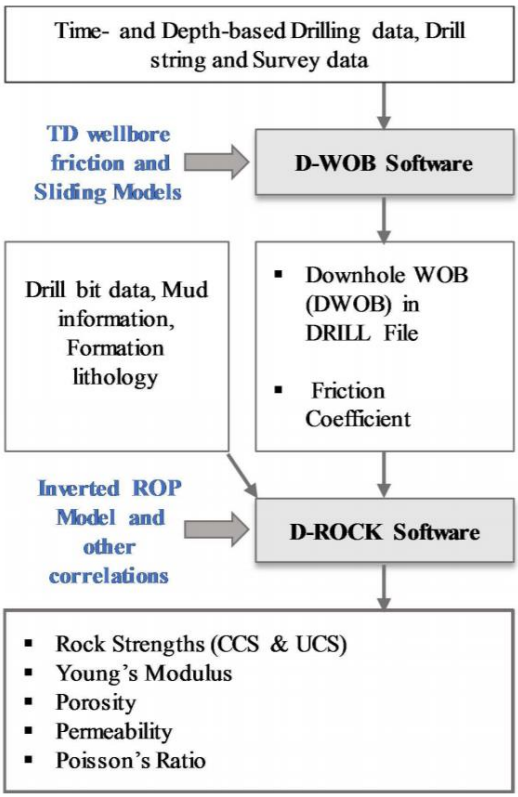

Figure 33: D-Series Software (M Tahmeen et al., 2017)

2.5.1 D-WOB Application to calculate friction coefficient and downhole weight-on-bit

Time and depth-based drilling data along with drill string information and survey data serve as the inputs into the D-WOB application. The wellbore friction torque and drag (T&D) model presented by Fazaelizadeh, et al. (2010) is used to calculate the coefficient of friction and effective downhole weight on bit (DWOB) from the surface measurements of WOB, hook load, surface applied RPM along with the wellbore survey measurements, standpipe pressure and drill string information. The wellbore friction models were developed by considering an element of the drill string in the

wellbore filled with drilling fluid and wellbore geometry (Fazaelizadeh et al., 2010). The following forces are considered on the drill string element: buoyed weight, axial tension, friction force and normal force perpendicular to the contact surface of the wellbore as shown in Figure 34 with *a* representing the drill string element with straight inclined section and *b* the curved section respectively (Mazeda Tahmeen et al., 2014) .

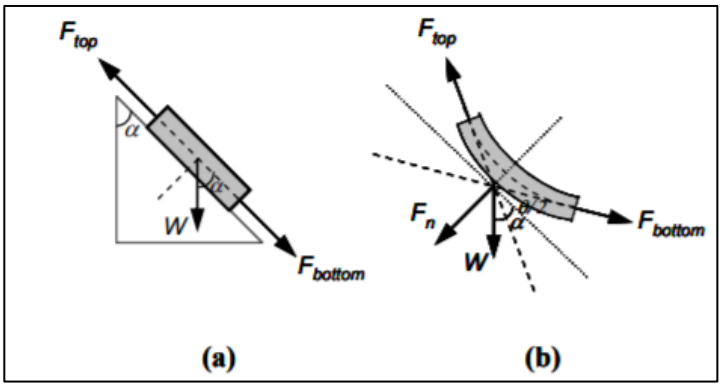

Figure 34: Force balance on drill string elements(Mazeda Tahmeen et al., 2014)

Equation 39 calculates the buoyed weight of the drill string element and equation 40 calculates the force balance on a drill string element when the bit is off bottom for a straight inclined section.

$$W = \beta w \Delta L \qquad \textit{Equation 39}$$

$$F_t = \beta w \Delta L(cos\alpha - \mu sin\alpha) + F_b \qquad \textit{Equation 40}$$

For a curved section in tension, the force balance on a drill string element is calculated by equations 41 and 42. For a curved section in compression, the force balance on a drill string element presented by Johancsik, et al. (1984) is calculated by equations 43 and 44. These equations are all used to calculate the coefficient of friction when the drill bit is off-bottom as well as the DWOB when the drill bit is on-bottom (M Tahmeen et al., 2017).

$$cos\theta = sin\alpha_t sin\alpha_b \, cos(\varphi_t - \varphi_b) + cos\alpha_t cos\alpha_b \qquad \textit{Equation 41}$$

$$F_t = \beta w \Delta L \left[\left(\frac{sin\alpha_t - sin\alpha_b}{\alpha_t - \alpha_b}\right) + \mu \frac{(cos\alpha_t - cos\alpha_b)}{\alpha_t - \alpha_b}\right] + F_b(e^{-\mu|\theta|}) \qquad \textit{Equation 42}$$

$$F_t = (\beta w \Delta L \left[cos\left(\frac{\alpha_t + \alpha_b}{2}\right)\right] - \mu F_n + F_b \qquad \textit{Equation 43}$$

$$F_n = \left[\left[F_b(\varphi_t - \varphi_b)\sin\left(\frac{\alpha_t + \alpha_b}{2}\right)\right]^2 + \left[F_b(\alpha_t - \alpha_b) \cdot (\beta \mathrm{w} \Delta \mathrm{L})\sin\left(\frac{\alpha_t + \alpha_b}{2}\right)\right]^2\right]^{\frac{1}{2}} \qquad \textit{Equation 44}$$

Using drilling data from a North American well applied to the lower Eagle Ford formation, Tahmeen et al (2017) performed an analysis on depths from 8,661 ft to 11,352 ft. The DWOB was calculated using the estimated friction coefficient, depth-based on-bottom drilling data and other required inputs. Figure 35 shows the difference between SWOB and calculated DWOB using the T&D model. The spikes in the weight on bit profile represent the higher WOB in the sliding mode. For the selected depth interval in the horizontal section, the friction coefficient was calibrated at each connection and the estimated values ranged from 0.09 to 0.18 (M Tahmeen et al., 2017). The calculated effective DWOB was observed to be around 77.6% of the surface measured WOB (SWOB) (M Tahmeen et al., 2017). The calculated DWOB values utilizing the T&D models were verified with the downhole weight on bit measurements obtained from the Copilot downhole tool, as shown in Figure 36 where spikes with higher SWOB can be seen.

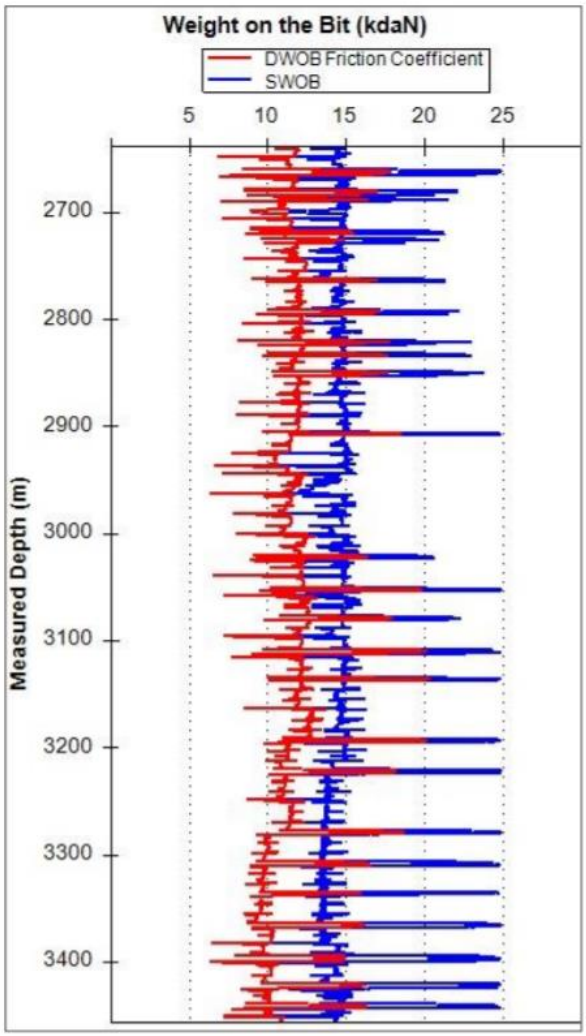

Figure 35: Downhole WOB (DWOB) profile from D-WOB software (M Tahmeen et al., 2017)

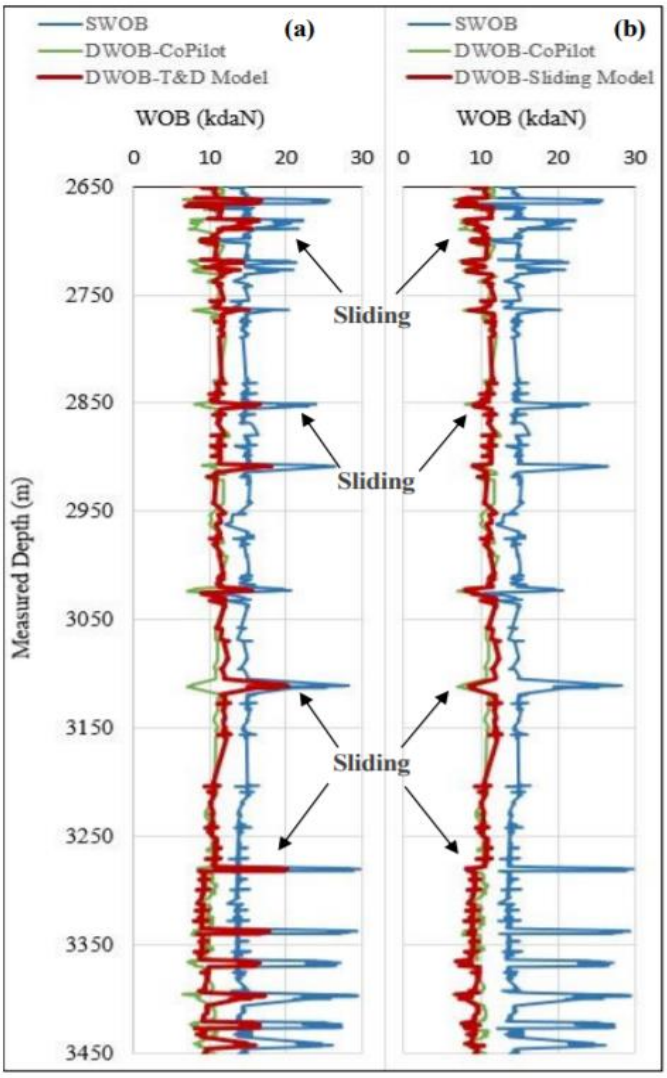

Figure 36: Comparison of calculated DWOB with the measurement from Copilot downhole tool (M Tahmeen et al., 2017)

2.5.2 D-ROCK Application to calculate CCS and UCS

The outputs from the D-WOB application along with drill bit data, mud information and formation lithology are the inputs to the D-ROCK software used to obtain the geomechanical property log. By inverting and arranging the ROP models for PDC and rollercone drill bits developed by Hareland and Nygaard (2007) to account for the effects of bit wear, drilling parameters such as pump flow rate and RPM, and drill bit cutting structure, the rock confined compressive strength (CCS) and UCS can be defined as equations 45 and 46 respectively (M Tahmeen et al., 2017).

Formation constants as, bs are calculated using laboratory triaxial test data on reservoir core samples and differ according to reservoir and formation type (M Tahmeen et al., 2017).

$$CCS = \left[\frac{ROP}{K \times DWOB^{b_1} \times RPM^{c_1} \times h_x \times W_f \times B_x}\right]^{\frac{1}{a_1}} \quad \textit{Equation 45}$$

$$UCS = \frac{CCS}{1 + a_s \times P_c^{b_s}} \quad \textit{Equation 46}$$

Using the same drilling data from the North American well applied to the lower Eagle Ford formation, the UCS was generated utilizing the DWOB calculated from the combined models for both rotary drilling and sliding mode. The UCS log generated from the data is depicted in Figure 37.

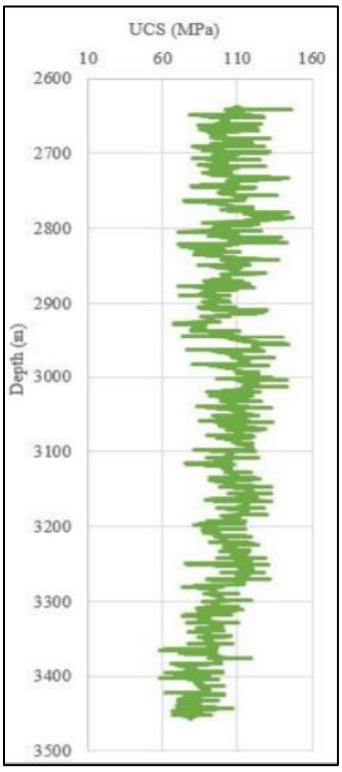

Figure 37: UCS and Young's modulus logs from D-ROCK software (M Tahmeen et al., 2017)

CHAPTER III

GARRETT WELL DATA

3.1 Background

The Garrett 1-36H well was drilled in 2013 by CLR. The drilling data was provided by CLR and contained all the required operational parameters for drilling presented in a time and depth-based format with intervals of either one foot or ten seconds. The Garrett well was drilled to a total depth (TD) of 17156 ft with a true vertical depth (TVD) of 14211 ft and a horizontal length that stretches out to 4980 ft. The Garrett well has a lateral length of 2695 ft and stands at an elevation of 1095 ft.

3.2 Location

The Garrett 1-36H is located in Stephens County, Oklahoma and was geographically placed in Section 36-2S-4W, drilling north in the downdip of the formation. The well card details of the Garrett well together with more location details can be found in Figures A1 to A5 of the Appendix. The Garrett oil well was targeted for the Caney Shale – a formation in the South-Central Oklahoma Oil Province (SCOOP) above the Woodford and Meramec formations near the Arbuckle Mountains. The Garrett landed in the lower zone of the Caney shale. Figure 38 shows a topographic vicinity map of the Garrett shown from ground elevation at the surface hole.

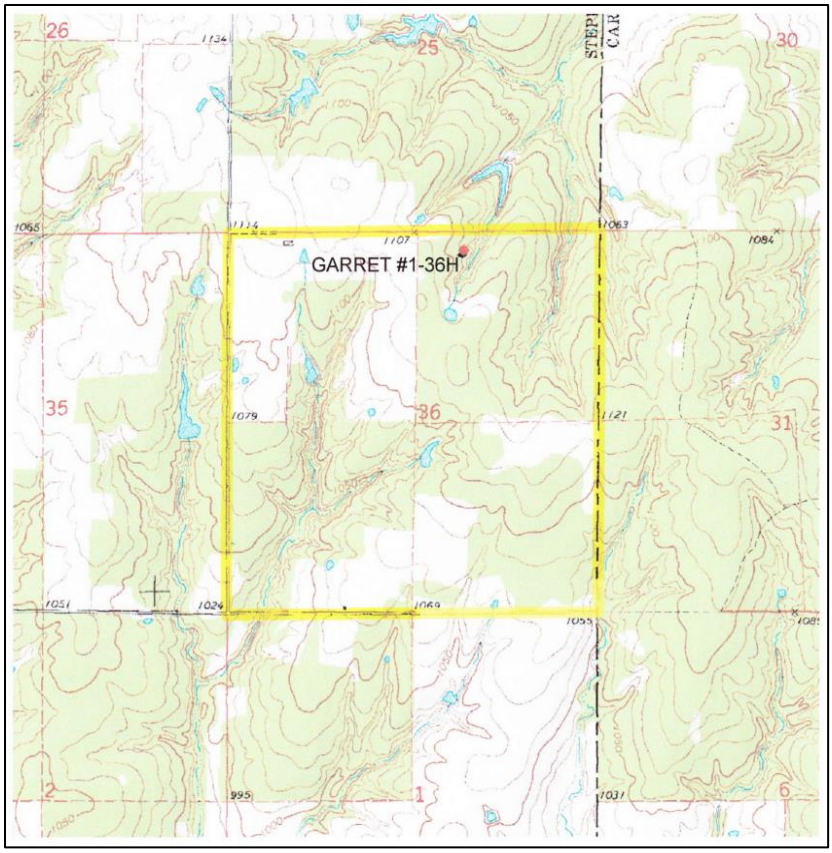

Figure 38: Topographic Vicinity Map of the Garrett Well (Image provided by CLR)

3.4 Well path and Target Reservoir

The Garrett well was drilled at an approximately 60° inclination from the 10,901 ft Kick Off Point (KOP). The Garrett was drilled with an original and 'sidetrack' section as represented in Figure 39. The sidetrack proved to have duplicate data from the original hole where quality control was necessary for data analysis. The sidetrack data was not used in the simulation and optimization process. Figure 40 shows a more traditional representation of a wellbore trajectory for the Garrett well without the sidetrack path. The target zone for the Garrett was in the Reservoir 3 zone of the Caney as displayed in Figure 41.

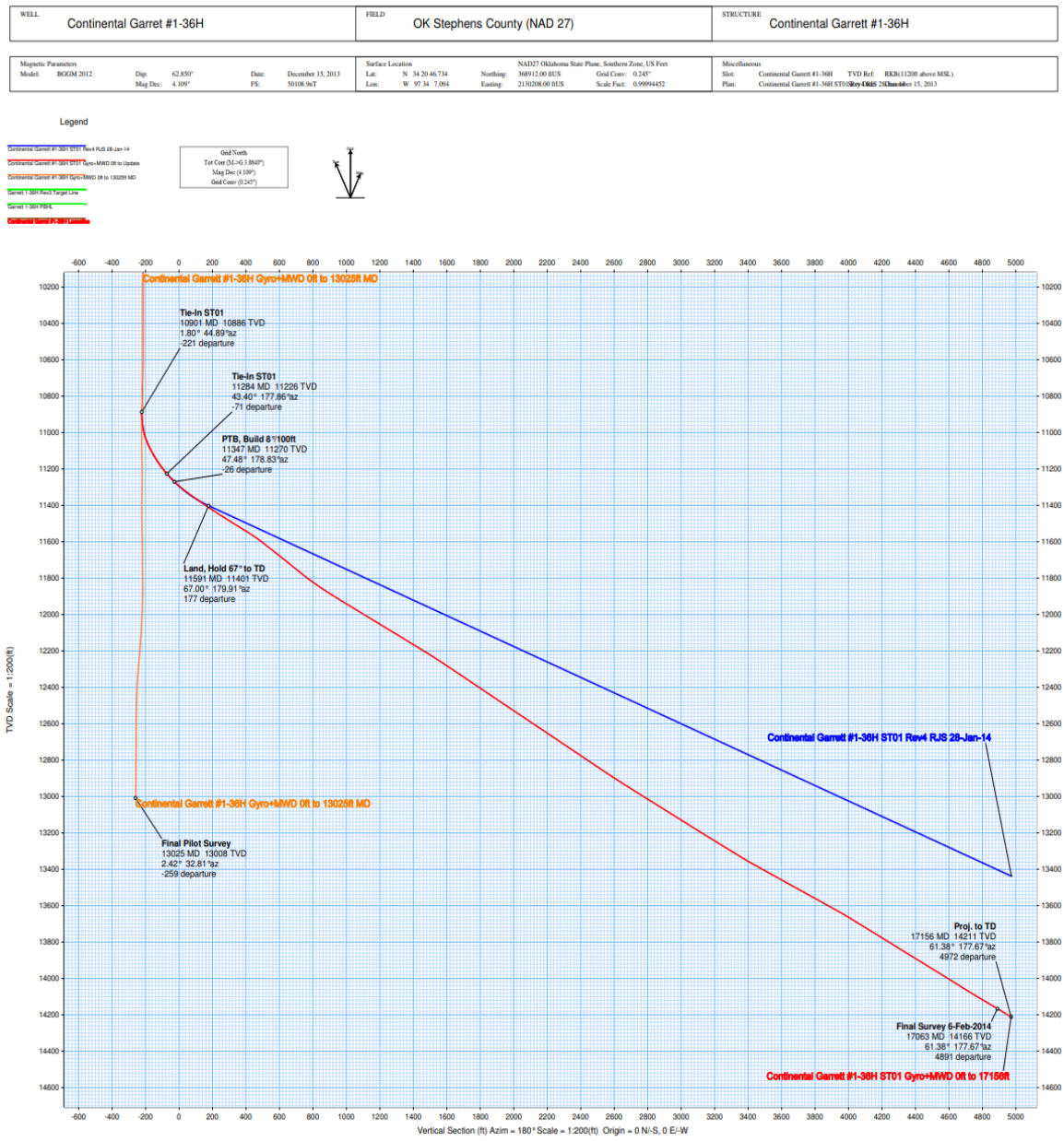

Figure 39: Garrett Well Path with Sidetrack

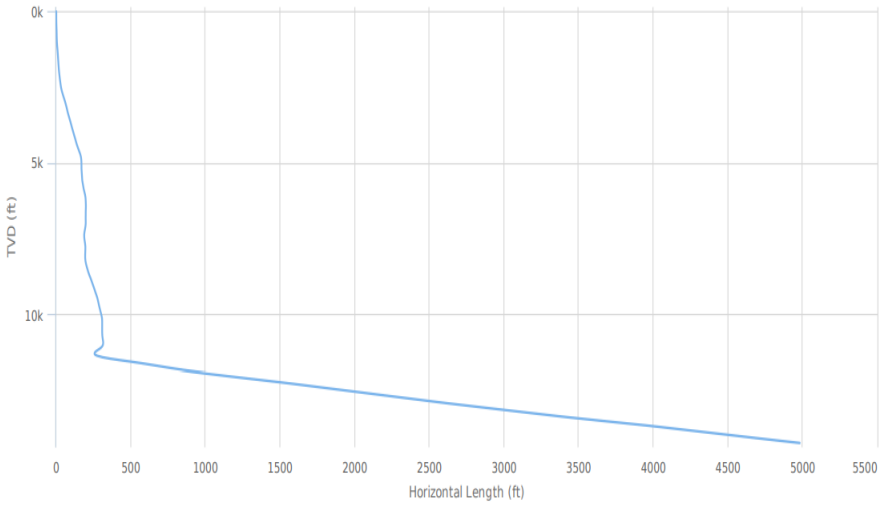

Figure 40: Garrett Wellbore Trajectory (Image provided by CLR)

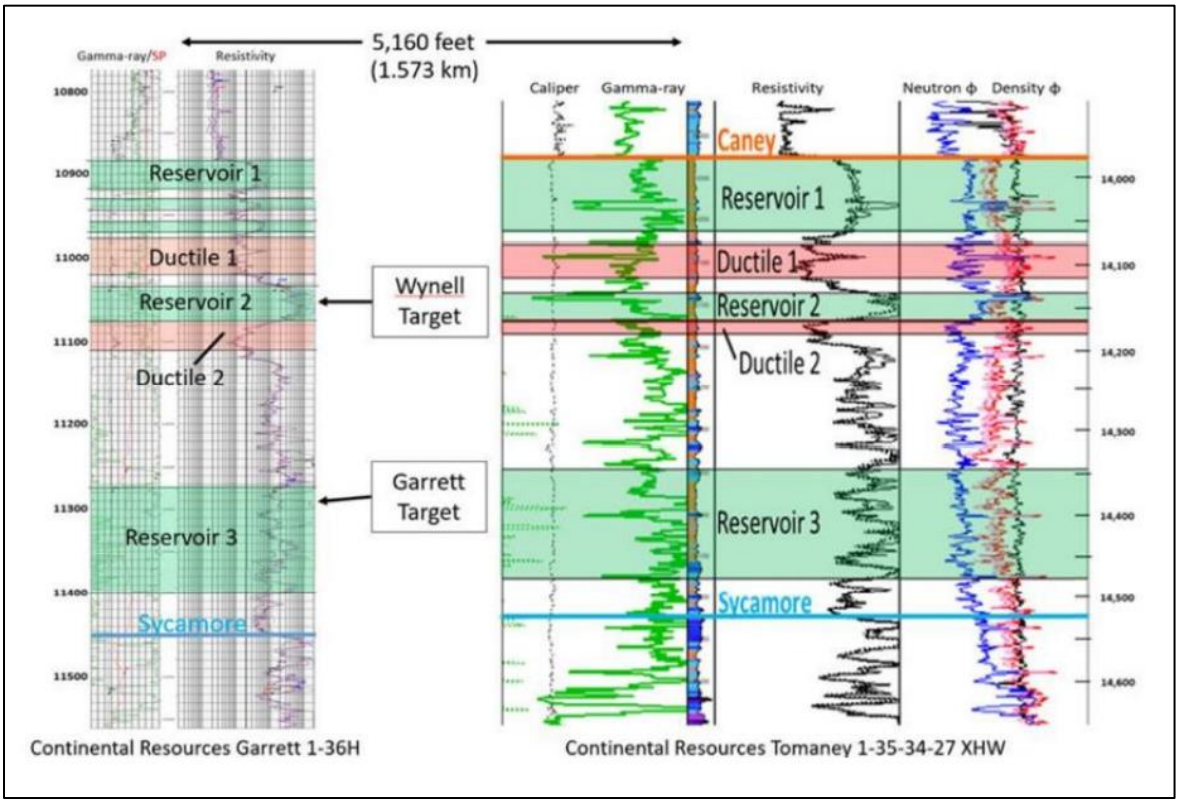

Figure 41: Target Reservoir for the Garrett well (Image provided by CLR)

CHAPTER IV

METHODOLOGY

4.1 Overview

In this chapter, a methodology is presented where the simulation and optimization steps are shown, as well as the inputs into the PDS and D-WOB software. The purpose of this chapter is to introduce the steps that were undertaken to calculate the friction coefficient and DWOB for the Garrett well using the D-WOB software and the steps to create the ARSL for the Gallaway from optimization using the PDS. The D-WOB application was used to generate DWOB from calculated friction coefficients based on equipment and torque and drag data. The D-Series software can also be used to calculate CCS, UCS, Young's Modulus (E), Poisson's ratio, permeability, and porosity and this data can later be utilized to better understand formation integrity, and characteristics along the horizontal section of the specific wellbore.

4.2 D-WOB Software

The D-WOB software was run to obtain the coefficient of friction and DWOB on a foot by foot basis for the Garrett well. The drilling data was first quality controlled to ensure accuracy and remove any redundant data. There is a quality control feature in D-WOB that allows for the depth-based file to be quality controlled. This feature enables an easier quality control job and smoother trends to be formed. Lower and upper bounds for WOB, RPM and ROP can be adjusted to ensure

the removal of values outside limits of reasonable extremity that are usually caused by inaccurate rig measuring or non-drilling time. The following inputs were necessary in order to run the software.

- Survey data (measured depth, TVD, inclination, and azimuth)
- Drilling data (date & time, bit depth, measured/hole depth, WOB, RPM, ROP, stand-pipe pressure, flow rate, differential pressure, and mud weight)
- Drill-string configuration (drill-string section lengths including BHA components)

The time and depth file contains information that enables the T&D models to be executed. The BHA file was provided by CLR where each BHA was described in detail. The components were averaged according to weight while the length was a summation of the full length of the BHA. The survey file included the depth, azimuth, inclination, and dogleg angle. Additional data that was necessary to run the application included hook weight, number of lines and sheave efficiency. These variables were found from provided drilling data where a 96% sheave efficiency and 10 lines were used. The hook weight of 40 klbf was found by plotting the hook load during connection. The data was then converted to text files and transferred into the DWOB software.

4.3 The Pason Drilling Simulator Input Files

The PDS uses three main inputs: a lithology file, a drilling parameters file, and a bit design parameters file. The lithology file contains all the required information about the formations from surface to TD. Table 11 shows an example of the formation types that are present within an input lithology file. The drill file contains all necessary operating parameters that are used to generate an ARSL. Table 12 shows the different drilling parameter requirements and the corresponding units required to run the simulation. The drilling data provided by CLR for the Garrett well contained all necessary operational parameters for drilling given in a time and depth-based format. These parameters consisted of the WOB, RPM, ROP, hook load, gamma ray, pump pressure and flow rate

among other operational parameters. Graphs showing depth versus the Garrett input WOB, RPM and ROP were plotted to help analyze fluctuations and trends as these can have an influence on the output ARSL. A graph showing the depth versus the input mud weight was also plotted. These graphs can be found in Figures A6 to A9 of the appendix. A survey report containing the measured depth, inclination, azimuth, and dogleg severity provided a drilling outline of the kickoff point and lateral depth. A bit file summarizing the bits used for each section, the section depths, bit nozzle sizes, bit grade, and reason for tripping was provided along with a BHA file that contained the mass per length of the BHA and individual components for the assembly. Table 13 shows an example of the input information required for each type of bit. The PDC bits require some geometry characteristics that can be added within the simulator. Lastly, the daily drilling reports were obtained which provide a day-to-day analysis of the drilling operation, mud weight details, lithology descriptions, and daily costs that provide a key understanding of the drilling data. Using all the drilling data and information provided, it was possible to quality control the data using excel before converting it into text files required as inputs into the PDS. By ensuring that all start and end depths were the same in all input files, bit depths were accurately input, the lithology summation at a specific depth didn't exceed 1 and all negative values were filtered from all input files, it was possible to run PDS without any errors.

Table 11:: Lithology Input File

Parameter	Unit	Explanation
MD	Meters	Measured depth
TD	Meters	True vertical depth
SAND	N/A	Fraction of sandstone in the formation
SHALE	N/A	Fraction of shale in the formation
LIME	N/A	Fraction of limestone in the formation
DOLO	N/A	Fraction of dolomite in the formation
SILI	N/A	Fraction of silicon in the formation
CONG	N/A	Fraction of conglomerate in the formation
COAL	N/A	Fraction of coal in the formation
NULL	N/A	Not used in current version
NULL	N/A	Not used in current version
NULL	N/A	Not used in current version
P.P.	g/cm^3	Pore pressure, gradient
PERM	N/A	Permeability, (1 = permeable, 0 = impermeable)

Table 12: Drilling Parameters Input File

Parameter	Unit	Explanation
MD	Meters	Measured depth
TD	Meters	True vertical depth
ROP	Meters per hour	Reported ROP
WOB	Tons	Weight on bit
RPM	Revolutions per minute	Rotary speed
GPM	Liters per minute	Flowrate
PV	Centi Poise	Plastic viscosity
MW	Specific Gravity	Mud weight
MUDTYPE	N/A	Water or oil based mud. (1 = oil, 0 = water)
DMODE	N/A	Indicates drilling mode. R = Rotary, S = Sliding and A = AutoBHA

Table 13: Bit Input File

Parameter	Unit	Explanation
[Info]		General info section
Version	N/A	File version
Well	N/A	Well name
Prepared by	N/A	Prepared by
Comment	N/A	**Optional**: Any comments, special considerations, etc.
[Bit serial no]	N/A	Manufactures bit serial
Bit Type	N/A	Bit type, PDC, TRI or NDB
IADC Code	N/A	IADC Code
Bit Diameter	Inch	Bit diameter
TVD In	Meter	True vertical start depth for bit run
TVD Out	Meter	True vertical end depth for bit run
MD In	Meter	Measured start depth for bit run
MD Out	Meter	Measured end depth for bit run
Wear In	N/A	Bit wear status before drilling as determined by IADC bit grading
Wear Out	N/A	Bit wear status after drilling as determined by IADC bit grading
Cost	US Dollars	Actual cost of drill bit
Cost DHM	US Dollars/ Day	Actual cost of motor rental per day
Manufacturer	N/A	Name of bit manufacturer
Bit Description	N/A	Bit description from manufacturer
Nozzle1..Nozzle8	1/32 Inch	**Required for TRI and PDC bits:** Description of the bits nozzle sizes, in 32's of an inch.If the bit has less than 8 nozzles, enter 0.0 in the remaining fields
Primary Number of Cutters	N/A	**Required for PDC bits:** Number of primary cutters on the bit.
Backup Number of Cutters	N/A	**Required for PDC bits:** Number of backup cutters on the bit.
Primary Cutter Size	Inch	**Required for PDC bits:** Size of primary cutters
Backup Cutter Size	Inch	**Required for PDC bits:** Size of backup cutters
Primary Backrake	Degree	**Required for PDC bits:** Backrake angle for primary cutters
Backup Backrake	Degree	**Required for PDC bits:** Backrake angle for backup cutters
Primary Siderake	Degree	**Required for PDC bits:** Siderake angle for primary cutters
Backup Siderake	Degree	**Required for PDC bits:** Siderake angle for backup cutters
Number of Blades	N/A	**Required for PDC bits:** Number of blades
Junk Slot Area	$Inch^2$	**Required for PDC bits:** Available area of bit for cuttings removal and cooling.
Thickness	1/64 Inch	**Required for PDC bits:** Thickness of the bits PDC layer.
Exposure	Inch	**Required for PDC bits:** The exposure of the PDC backup cutters
Distance	Inch	**Required for PDC bits:** The horizontal distance between the primary and backup cutters on the bit
Number of Diamonds	N/A	**Required for NDB bits:** Number of diamonds
Diamond Size	Inch	**Required for NDB bits:** Size of diamonds.
Pump Off Area	$Inch^2$	**Required for NDB bits:** Pump off area
Apparent Flow Area	$Inch^2$	**Required for NDB bits:** Apparent flow area

4.3.1 Formation Tops

Formation tops, bit information and BHA details were provided from meetings held with CLR. Formation tops for both Garrett and Gallaway are listed in Table 14. By adjusting formation tops accordingly within the PDS, it was possible to correlate the Garrett ARSL to the Gallaway ARSL to match the provided formation top depths for the Gallaway. This process involved stretching and shrinking certain geological formations to create an accurate depiction of the Gallaway strength log.

Table 14: Formation Tops for the Garrett and Gallaway Wells

Estimated Tops (ft)			
Garrett Well		Gallaway Well	
Tops	TVD (pilot)	Est. Tops	Est. MD
HOXBAR	2148	HOXBAR	3222
DEESE	4298	DEESE	5505
UP. FUSULINID	4559	UP. FUSULINID	6334
FUSULINID	4960	FUSULINID	6471
TUSSY	5491	TUSSY	6935
ATOKA	6552	TUSSY BASE	7607
DORNICK HILLS	7300	ATOKA	9092
SPRINGER	8239	DORNICK HILLS	9928
HUMPHRIES	8353	DORNICK HILLS BASE	10400
SIMS	8742	SPRINGER	11105
GOODWIN	9263	HUMPHRIES	11275
FALSE CANEY	10618	SIMS	11595
CANEY	10870	GOODWIN	12471
		GOODWIN base	12581
		FALSE CANEY	13540
		CANEY	14095

4.3.2 Mud Weight Program (MWP)

Mud weights, presented in a time and depth-based format with intervals of either one foot or ten seconds, from the Garrett well were used to create a mud weight program which was used in the simulation of the Gallaway well. Figure A7 in the Appendix shows the mud weights used for the optimization process. The proposed mud weights for the Gallaway as provided by CLR are shown in Table 15 below.

Table 15: Proposed Mud Weights

MUD PROGRAM

Depth	Type	Weight	Remarks
0 ' - 1500 '	Spud Mud	8.4-8.8	Spud Mud
1500 ' - 13600 '	LSLD	9.3-10.0	FV: 38-50, NC- ≤4, LCM: as needed
13600 ' - TD '	80/20 Diesel	10.3-15	FV: 50-75, ≤4, LCM: poss. losses in ********

4.3.3 Bit Design and Parameters

The simulations were run with a total of five bits from surface to TD. The Garrett bits which were used as the initial bit inputs are shown in Table A1 in the appendix. The proposed bits for the

Gallaway later replaced the Garrett bits to suit the new well to be drilled. The specific bits used in optimizing the Gallaway are shown in Table 16 below. These bit specifications were provided by CLR. A more detailed sectional analysis as well as corresponding bits that were used for each section will be discussed in chapter 5.

Table 16: Bits used in the Gallaway

Bit ID	**Bit size**	**Nozzle size (in)**
Baker HC 6055	17.5	7x12
Baker 506	12.25	6x16
Baker 405	12.25	5x13
Reed 713	8.75	5x13, 2x14

4.3.4 Motor RPM

A motor RPM was incorporated in the optimization process of the 12.25'' and 8.75'' sections. A 0.08 revolutions per gallon (rpg) motor was used in the 12.25" section and a 0.2 rpg motor was used in the 8.75" section in the turn (build section). The motor RPM was used with flowrate to determine the bit RPM in sliding and rotating mode which is necessary in order to accurately optimize the sections based on the drilling mode used. The motor RPM was added to the surface RPM to get the bit total RPM. By knowing both the optimized bit RPM and motor RPM, the surface RPM was calculated using Equation 40.

$$Bit\ RPM = SurfaceRPM + Motor\ RPM \qquad \textit{Equation 47}$$

CHAPTER V

RESULTS

5.1 Overview

The following section presents results obtained from the D-WOB software and PDS optimization. The outputs for both the PDS and D-WOB software are discussed and outlined in this chapter. Results from the D-WOB software showing the coefficient of friction, D-WOB and SWOB for the Garrett well will also be discussed and results presented. A completely optimized drilling program for the Gallaway well will be presented in this chapter and a comprehensive and detailed sectional analysis will be outlined, and results explained. A discussion section explaining other optimization alternatives is explained and lastly, a recommendation for the Gallaway drilling plan will be drawn from the optimization results.

5.2 Garrett Well D-WOB Results

The D-WOB software was run to find the coefficient of friction and DWOB for the Garrett well. Drilling data from the Garrett lateral section was used to analyze the results. The D-WOB software uses time-based data when the drillstring is lowered before touching the bottom of the hole between connections. As the drillstring is not touching the bottom and WOB is zero, the friction coefficient can be obtained iteratively using the hook load by subtracting the hook weight and the sheave friction and then comparing it to the calculated buoyant drill string weight minus the friction component. The friction component is then determined iteratively by taking the survey and string

weight components into account. The wellbore friction for the Garrett lateral is presented in Figure 42 and shows a graphical representation of the average friction that occurs along that wellbore as obtained from D-WOB. The friction coefficient varies as the well approaches the lateral. This deviation can cause a spike in the friction which can be observed in the graph at 12,000ft. The comparison plot consisting of the DWOB and SWOB plotted side by side is also shown in Figure 42. These plots were used to address the difference in WOB that is observed throughout the wellbore which is approximately 5-10 klbf. For a vertical well, this difference is zero as there is a 100% weight transfer from the surface to the bit.

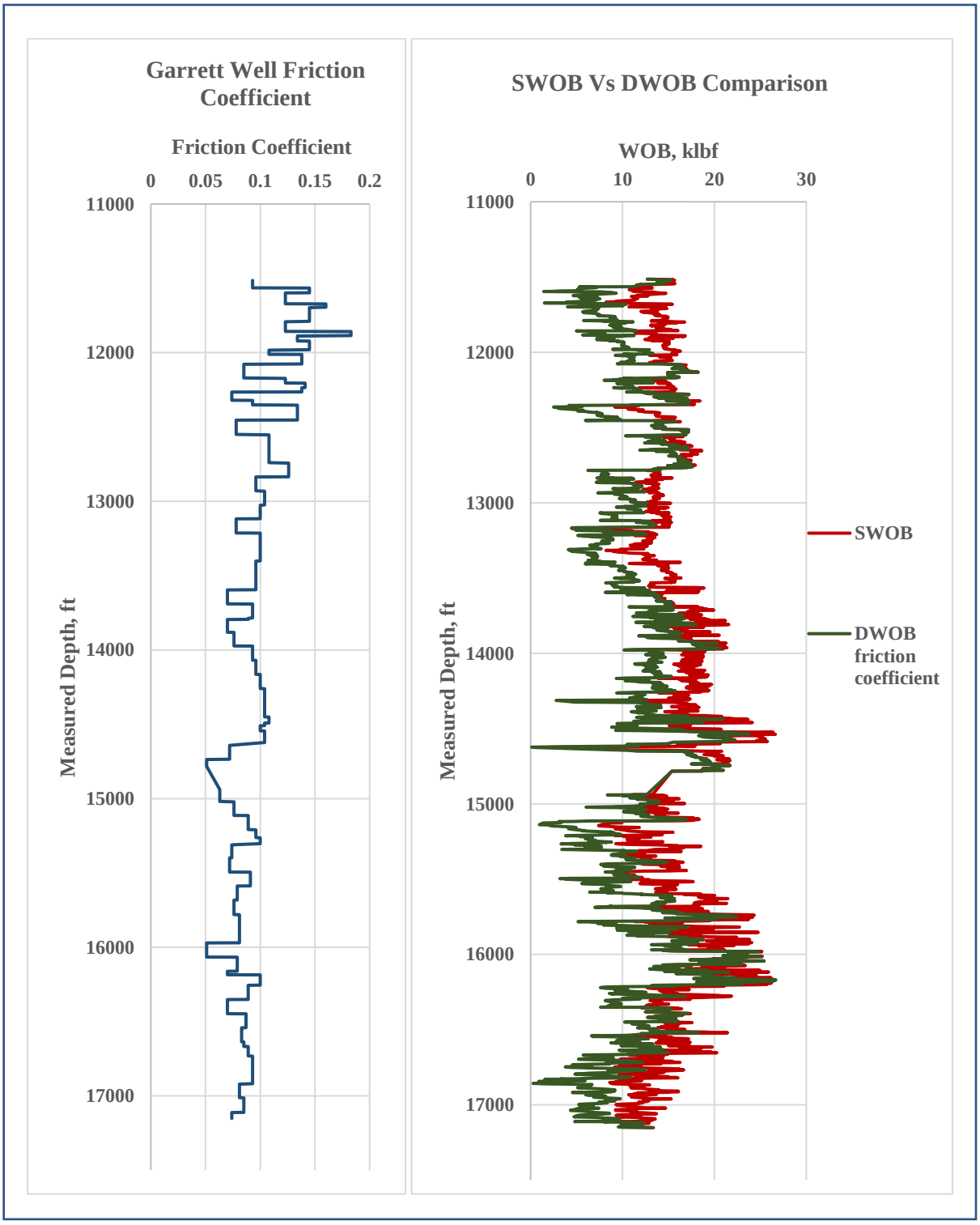

Figure 42: Friction Coefficient and (SWOB Vs DWOB)

5.3 Pason Drilling Simulator Results

A detailed simulation and optimization approach implemented for the Gallaway is outlined below for each section. Figure 43 shows a plot of the Garrett well before the optimization process which shows the original ARSL before any alterations.

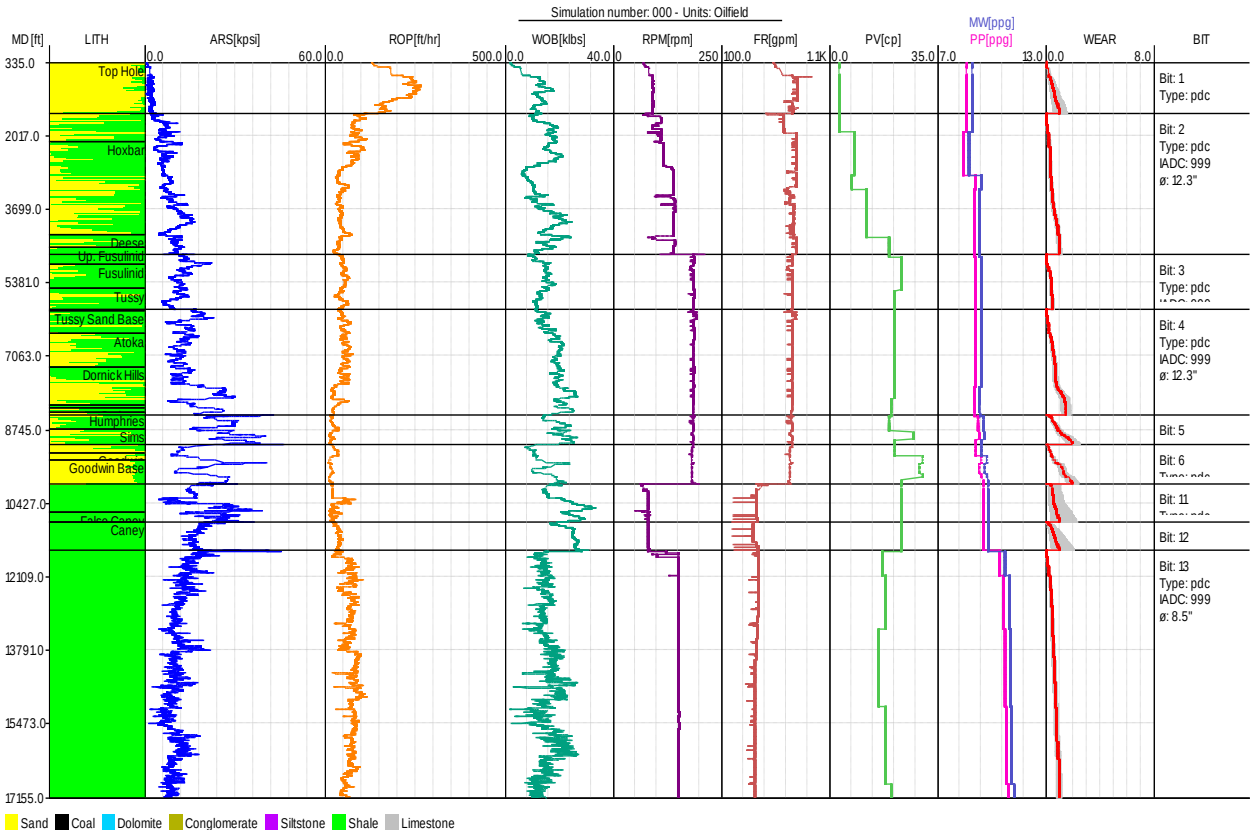

Figure 43: Original Garrett Simulation window

Optimized results for the Gallaway showing the generated ARSL are depicted in Figure 44. Figure 45 shows the finalized simulation sectional parameters. A total rotating time of 394 hrs (16 days) was seen for the simulation using a total of 5 bits for the entire well and 150 hrs was seen up to KOP. The Gallaway well kicks off 2,960 ft further down than the Garrett at 13,861 ft. A total optimized rotating time of 150 hrs up to KOP could mean a reduction in rotating time and cost per foot for the Gallaway well.

17.5’’ Section

Optimization in the 17.5’’ section resulted in an average ROP of 167 ft/hr. Controlled drilling was advised for this section due to potential hole cleaning issues when drilling faster.

12.25’’ Section

Two HC-bits with tier 1 cutters were used to drill the 12.25’’ section. This section was simulated using a WOB range of 35-60 klbs at an average ROP of 58 ft/hr and 37 ft/hr for bit 1 and bit 2 respectively. A 0.08 rpg motor was also used in this section which resulted in a motor RPM of 60 RPM at a mud flowrate of 750 GPM for the entire section and a recommended surface RPM from 10 to 25 RPM.

8.75’’ Section (Turn)

The Gallaway well kicks off at 13,861 ft with an estimated 85% sliding and 15% rotating. An HC 405 bit was used throughout this section with a simulated downhole WOB of 25 klbs resulting in an average ROP of 54 ft/hr. Estimated averaged parameters were applied in rotating mode since the prediction of sliding depths is impossible. It was advised to maintain the same differential pressure in sliding mode as when rotating with the 25 klbs for the entire section. A 0.2 rpg motor was also used throughout the section which yielded an 85 motor RPM at a mud flowrate of 425 GPM and a recommended 20 RPM at the surface.

8.75’’ Section (Lateral)

An RH-713 bit with tier 1 cutters was used in the lateral with an estimated 95% rotating and 5% sliding. Downhole WOB in rotating mode was simulated with 20 klbs at an RPM of 195 resulting in an average ROP of 72 ft/hr. A 0.2 rpg motor was also used throughout the section which yielded 85 RPM at a mud flowrate of 425 GPM and a recommended 110 RPM at surface.

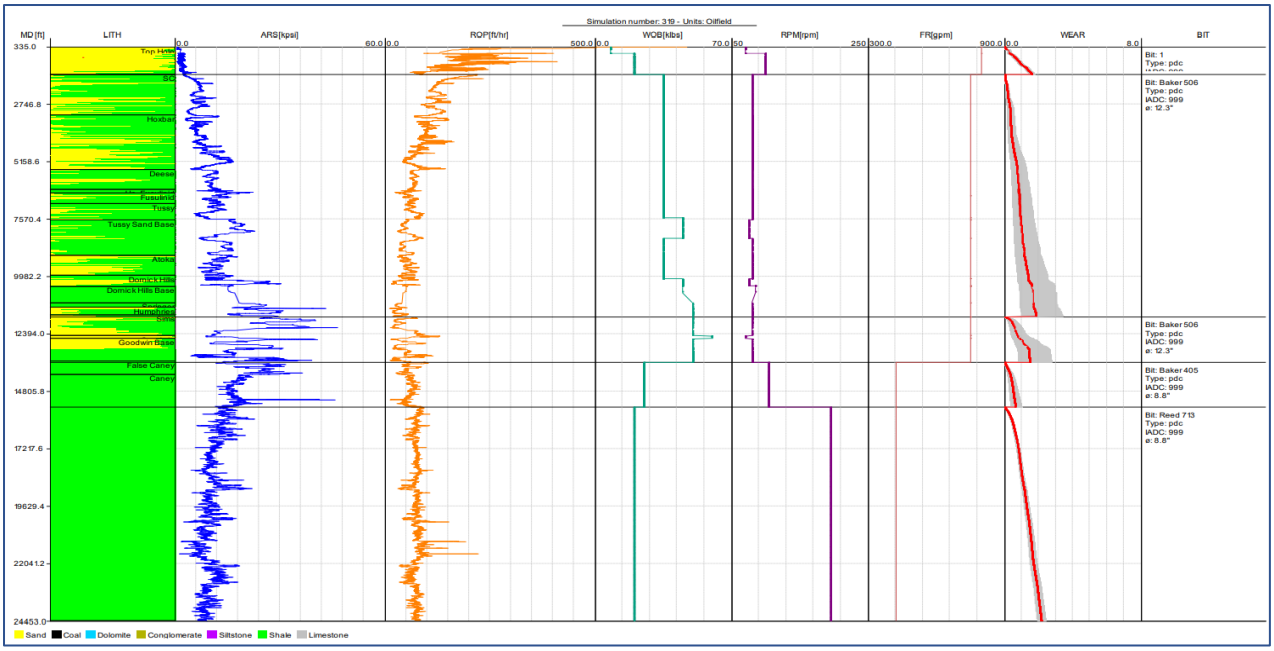

Figure 44: PDS Optimized Results

Bit #	Bit Size	Bit ID	Nozzle Size	Depth In	Depth Out	Interval Section	WOB	Surface RPM	Motor RPM	Bit RPM	MW	GPM	Section Sim.	Avg. ROP	Avg. IADC Wear Out	Bit Hours
1	17.5	Baker HC6055	7x12	335	620	285	8	70	0	70	8.4	800	204		0.3	
1	17.5	Baker HC6055	7x12	620	1520	900	20	100	0	100	8.4	800	158	167	1.6	7
2	12.25	Baker 506	6x16	1521	6610.5	5089.5	35	20	60	80	9.3	750	85		0.8	
2	12.25	Baker 506	6x16	6610.5	7530	919.5	35	20	60	80	9.3	750	63		0.9	
2	12.25	Baker 506	6x16	7530	7607	77	45	20	60	80	9.3	750	62		1	
2	12.25	Baker 506	6x16	7607	8400	793	45	15	60	75	9.3	750	48		1.1	
2	12.25	Baker 506	6x16	8400	10100	1700	35	20	60	80	9.3	750	48		1.4	
2	12.25	Baker 506	6x16	10100	10380	280	45	15	60	75	9.3	750	30		1.6	
2	12.25	Baker 506	6x16	10380	10400	20	45	25	60	85	9.3	750	29		1.6	
2	12.25	Baker 506	6x16	10400	11100	700	45	25	60	85	9.3	750	45		1.7	
2	12.25	Baker 506	6x16	11100	11700	600	50	20	60	80	9.3	750	27	58	1.9	175
3	12.25	Baker 506	6x16	11700	12471	771	50	20	60	80	9.3	750	35		0.8	
3	12.25	Baker 506	6x16	12471	12581	110	60	10	60	70	9.3	750	49		0.9	
3	12.25	Baker 506	6x16	12581	13600	1019	50	20	60	80	9.3	750	38	37	1.5	51
4	8.75	Baker 405	5x13	13600	15486	1886	25	20	85	105	10.3	425	54	54	0.6	35
5	8.75	Reed 713	5x13, 2x14	15486	24453	8967	20	110	85	195	10.3	425	72	72	2.2	125
															Avg Well ROP	61
															Time	394

Figure 45: Detailed Simulation Sectional Parameter Results

5.4 Discussion

A separate set of simulations were made using three bits in the 12.25'' section instead of two bits. The addition of the new bit resulted in a total of six bits used for the entire well. This was done to run a comparison and see how three bits in the 12.25'' section would affect the average well ROP and total rotating time. The use of an extra bit in the 12.25'' section resulted in a 52 hr reduction in rotating time and a 9 ft/hr increase in average ROP but also added in trip time and bit cost. Figure 46 shows a total well time comparison between two and three bits in the 12.25'' section. Table 17 summarizes the ROP, and total rotating time observed for the two scenarios. The optimized results for a total of six bits showing the generated ARSL are depicted in Figure 47. Figure 48 shows the finalized simulation sectional parameters. A total rotating time of 342 hrs (14 days) was observed for the simulation using a total of 6 bits.

Table 17: Two vs Three bits summary

	2 Bits	3 Bits
Average ROP, ft/hr	61	70
Time, hrs	394	342

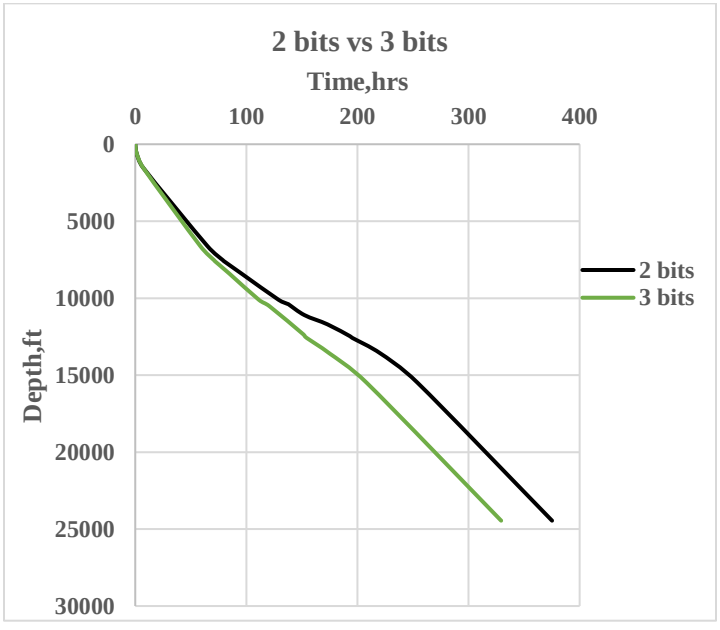

Figure 46: Two vs Three bits time comparison

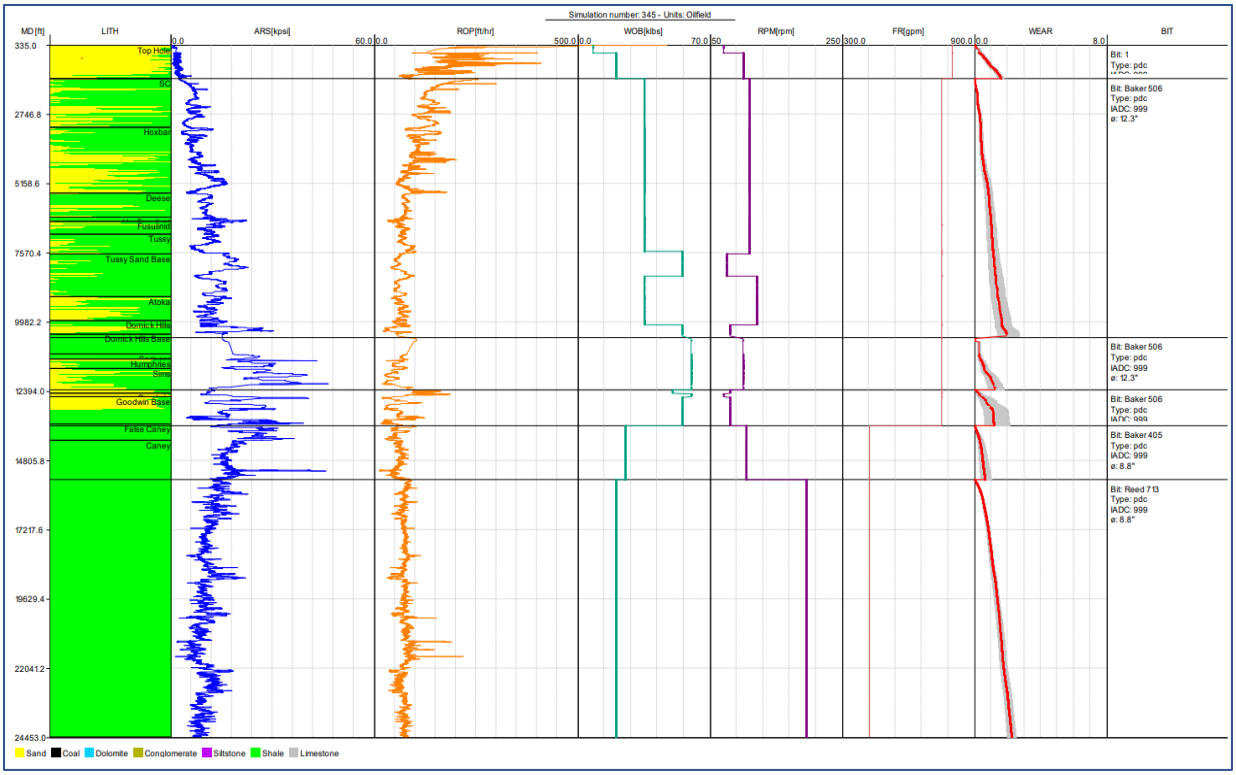

Figure 47: PDS Optimized Results for six bits

Bit #	Bit Size	Bit ID	Nozzle Size	Depth In	Depth Out	Interval Section	WOB	Surface RPM	Motor RPM	Bit RPM	MW	GPM	Section Sim.	Avg. ROP	Avg. IADC Wear Out	Bit Hours
1	17.5	Baker HC6055	7x12	335	620	285	8	70	0	70	8.4	800	204		0.3	
1	17.5	Baker HC6055	7x12	620	1520	900	20	100	0	100	8.4	800	158	167	1.6	7
2	12.25	Baker 506	6x16	1521	6610.5	5089.5	35	50	60	110	9.3	750	96		1	
2	12.25	Baker 506	6x16	6610.5	7530	919.5	35	50	60	110	9.3	750	72		1.1	
2	12.25	Baker 506	6x16	7530	7607	77	55	50	60	110	9.3	750	81		1.1	
2	12.25	Baker 506	6x16	7607	8400	793	55	15	60	75	9.3	750	59		1.2	
2	12.25	Baker 506	6x16	8400	10100	1700	35	60	60	120	9.3	750	61		1.7	
2	12.25	Baker 506	6x16	10100	10530	430	55	20	60	80	9.3	750	42	76	1.9	118
3	12.25	Baker 506	6x16	10530	12360	1830	60	40	60	100	9.3	750	57	57	1.2	32
4	12.25	Baker 506	6x16	12360	12471	111	50	20	60	80	9.3	750	93		0.2	
4	12.25	Baker 506	6x16	12471	12581	110	60	10	60	70	9.3	750	63		0.5	
4	12.25	Baker 506	6x16	12581	13600	1019	55	20	60	80	9.3	750	47	50	1.1	25
5	8.75	Baker 405	5x13	13600	15486	1886	25	20	85	105	10.3	425	54	54	0.6	35
6	8.75	Reed 713	5x13, 2x14	15486	24453	8967	20	110	85	195	10.3	425	72	72	2.2	125
															Avg Well ROP	70
															Time	342

Figure 48: Finalized simulation sectional parameters for six bits

5.5 Recommendation

The concern with using three bits is that a higher WOB is required in longer intervals where torquing up the Down Hole Motor (DHM) could be an issue. Even though a higher ROP was generated when using three bits which in turn lessened the total rotating time, adding the trip time and bit cost still makes the two cases a wash. Due to the additional trip cost, bit cost and potential for DHM stalling at higher WOB over longer periods, 2 bits in the 12.25” section seems like the most reasonable option.

CHAPTER VI

CONCLUSIONS

In the thesis herein, an ARSL was generated using the PDS and drilling data from an adjacent offset well (Garrett) to plan for a new well (Gallaway) to be drilled. Alongside the PDS, the D-WOB software was run to calculate the friction coefficient and DWOB of the Garrett well.

The D-WOB software can be used to run a comparison between the DWOB and SWOB and verify the effect of friction along the wellbore. The PDS has the capacity to simulate and optimize a drilling process and generate an ARSL completely based on offset well data. This research shows how the use of the drilling ROP models (PDS), and T&D (D-WOB) can be used to predict both ROP and rock strength for upcoming wells.

A recommendation based on the optimization procedure and equipment limitations was drawn and indicates that the use of two bits in the 12.25" was the most reasonable and cost-effective option. This research further proves that the ROP and DWOB are critical variables in determining an efficient and cost-effective drilling operation. Increasing the WOB improves drilling efficiency, however, it is critical to increase the WOB and reduce the RPM when encountering abrasive zones to avoid excessive wearing of the bit.

CHAPTER VII

FUTURE WORK AND RECOMMENDATIONS

The use of the drilling simulator creates more avenues for data validation and verification. The ARSL log generated by the PDS will be used to verify and validate the accuracy of the software by overlaying the adjusted Garrett ARSL with the ARSL that will be generated from Gallaway drilling data and adjusted DWOB from the D-WOB software. The strength log generated from the Gallaway by the PDS should match the strength log generated from the Garrett if the provided information on formation tops, drilling data and bit designs by CLR are correct. This process will start as soon as the drilling data has been provided by CLR. The ARSL generated for the Gallaway can later be used to plan and simulate for future wells to obtain an accelerated learning curve for wells to be drilled in the Caney formation in SW Oklahoma.

REFERENCES

Al Dushaishi. (Fall 2020). PETE 4313, *Lecture 4: Bit Types*. Oklahoma State University

Barzegar, M., Gharehdash, S., & Osanloo, M. (2014). Damage Analysis in Rock Rotary Tricones Bit–A Case Study. In *Mine Planning and Equipment Selection* (pp. 261-269): Springer.
DOI: 10.1007/978-3-319-02678-7_27

Bratli, R., Hareland, G., Stene, F., Dunsaed, G., & Gjelstad, G. (1997). *Drilling optimization software verified in the North Sea.* Paper presented at the Latin American and Caribbean Petroleum Engineering Conference.
doi.org/10.2118/39007-MS

Eren, T., & Ozbayoglu, M. E. (2010). *Real time optimization of drilling parameters during drilling operations.* Paper presented at the SPE oil and gas India conference and exhibition.
doi.org/10.2118/129126-MS

Fazaelizadeh, M., Hareland, G., & Aadnoy, B. S. (2010). Application of new 3-D analytical model for directional wellbore friction. *Modern applied science, 4*(2), 2.
https://www.rocsoltech.com/wp-content/uploads/2018/09/Application-of-New-3-D-Analytical-Model-for-Directional-Wellbore-Friction-MAS-Journal.pdf

Gjelstad, G., Hareland, G., Nikolaisen, K., & Bratli, R. (1998). *The method of reducing drilling costs more than 50 percent.* Paper presented at the SPE/ISRM Rock Mechanics in Petroleum Engineering.
doi.org/10.2118/47342-MS

Hareland, G., & Nygaard, R. (2007). *Calculating unconfined rock strength from drilling data.* Paper presented at the 1st Canada-US Rock Mechanics Symposium.
https://onepetro.org/ARMACUSRMS/proceedings/ARMA07/All-ARMA07/ARMA-07-214/116437

Hegde, C., & Gray, K. (2018). Evaluation of coupled machine learning models for drilling optimization. *Journal of Natural Gas Science and Engineering, 56*, 397-407.
doi:10.1016/j.jngse.2018.06.00610.1016/j.jngse.2018.06.00

Hossain, M. E. (2015). Drilling Costs Estimation for Hydrocarbon Wells. *Journal of Sustainable Energy Engineering, 3*(1), 3-32. doi:10.7569/jsee.2014.62952010.7569/jsee.2014.629520

Johancsik, C., Friesen, D., & Dawson, R. (1984). Torque and drag in directional wells-prediction and measurement. *Journal of Petroleum Technology, 36*(06), 987-992. doi:10.2118/11380-PA10.2118/11380-PA

Kerkar, P. B., Hareland, G., Fonseca, E. R., & Hackbarth, C. J. (2014). *Estimation of rock compressive strength using downhole weight-on-bit and drilling models.* Paper presented at the International Petroleum Technology Conference. doi.org/10.2523/IPTC-17447-MS

Lummus, J. L. (1970). Drilling Optimization. *Journal of Petroleum Technology, 22*(11), 1379-1388. doi:10.2118/2744-pa10.2118/2744-pa

Millheim, K. K. (1983). *An engineering simulator for drilling: part I.* Paper presented at the SPE Annual Technical Conference and Exhibition. DOI: https://doi.org/10.2118/12210-MS

Millheim, K. K., & Gaebler, T. (1999). *Virtual experience simulation for drilling-the concept.* Paper presented at the SPE/IADC drilling conference. doi.org/10.2118/52803-MS

Mofrad, M. A. (2005). Entire Hole Section Optimization with the PDS. https://www.researchgate.net/publication/334045680_Entire_Hole_Section_Optimization_with_the_PDS

Rampersad, P., Hareland, G., & Boonyapaluk, P. (1994). *Drilling optimization using drilling data and available technology.* Paper presented at the SPE Latin America/Caribbean Petroleum Engineering Conference. doi.org/10.2118/27034-MS

Tahmeen, M., Hareland, G., & Aadnoy, B. S. (2014). *Real-time software to estimate friction coefficient and downhole weight on bit during drilling of horizontal wells.* Paper presented at the International Conference on Offshore Mechanics and Arctic Engineering. doi.org/10.1115/OMAE2014-24620

Tahmeen, M., Love, J., Rashidi, B., & Hareland, G. (2017). *Complete geomechanical property log from drilling data in unconventional horizontal wells.* Paper presented at the 51st US Rock Mechanics/Geomechanics Symposium. https://onepetro.org/ARMAUSRMS/proceedings/ARMA17/All-ARMA17/ARMA-2017-0591/124518

Warren, T. (1984). *Penetration Rate Performance of Roller Cone Bits, paper SPE 13259.* Paper presented at the 59th Annual Technical Conference and Exhibition.

Wu, A., & Hareland, G. (2012). *Calculation of Friction Coefficient and Downhole Weight on Bit with Finite Element Analysis of Drillstring.* Paper presented at the 46th US Rock Mechanics/Geomechanics Symposium.

https://www.bakerhughes.com/drilling/drill-bits/pdc-drill-bits

http://duratechequip.com/products/pdc-bits/

https://www.clr.com/

APPENDICES

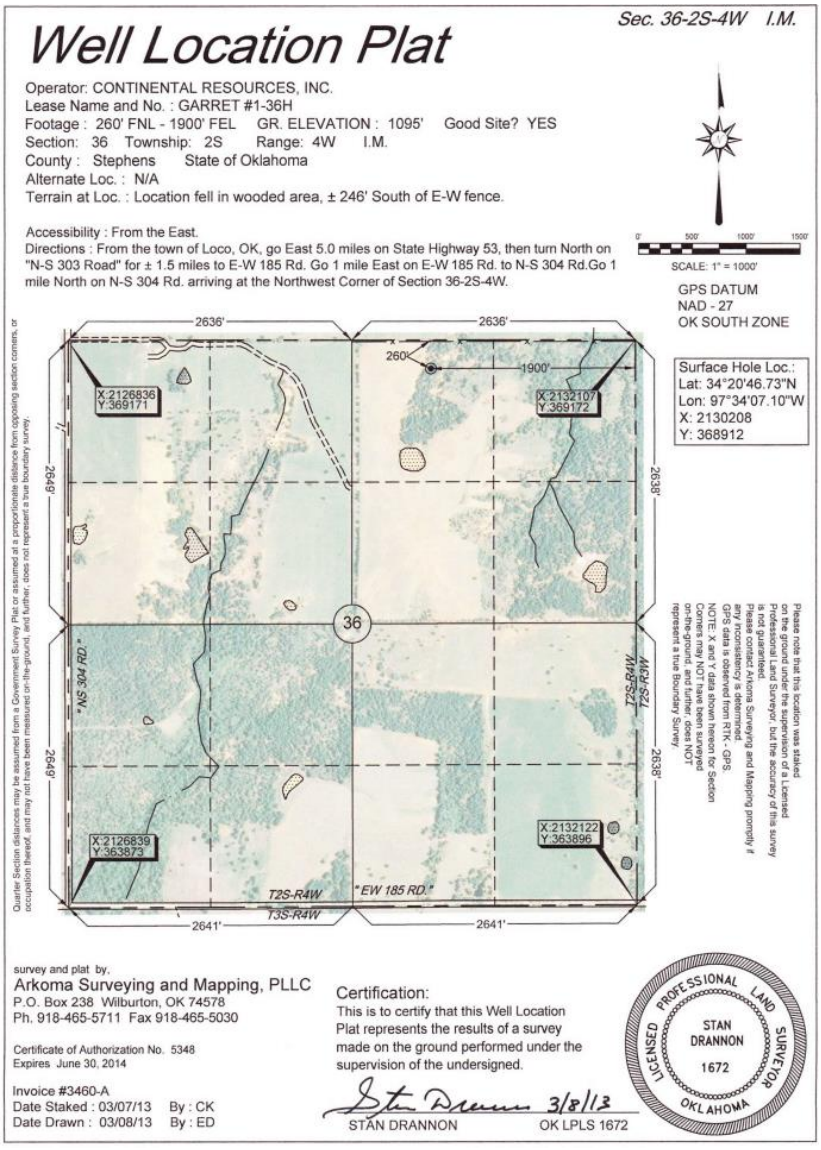

Figure A1: Well Location Plat

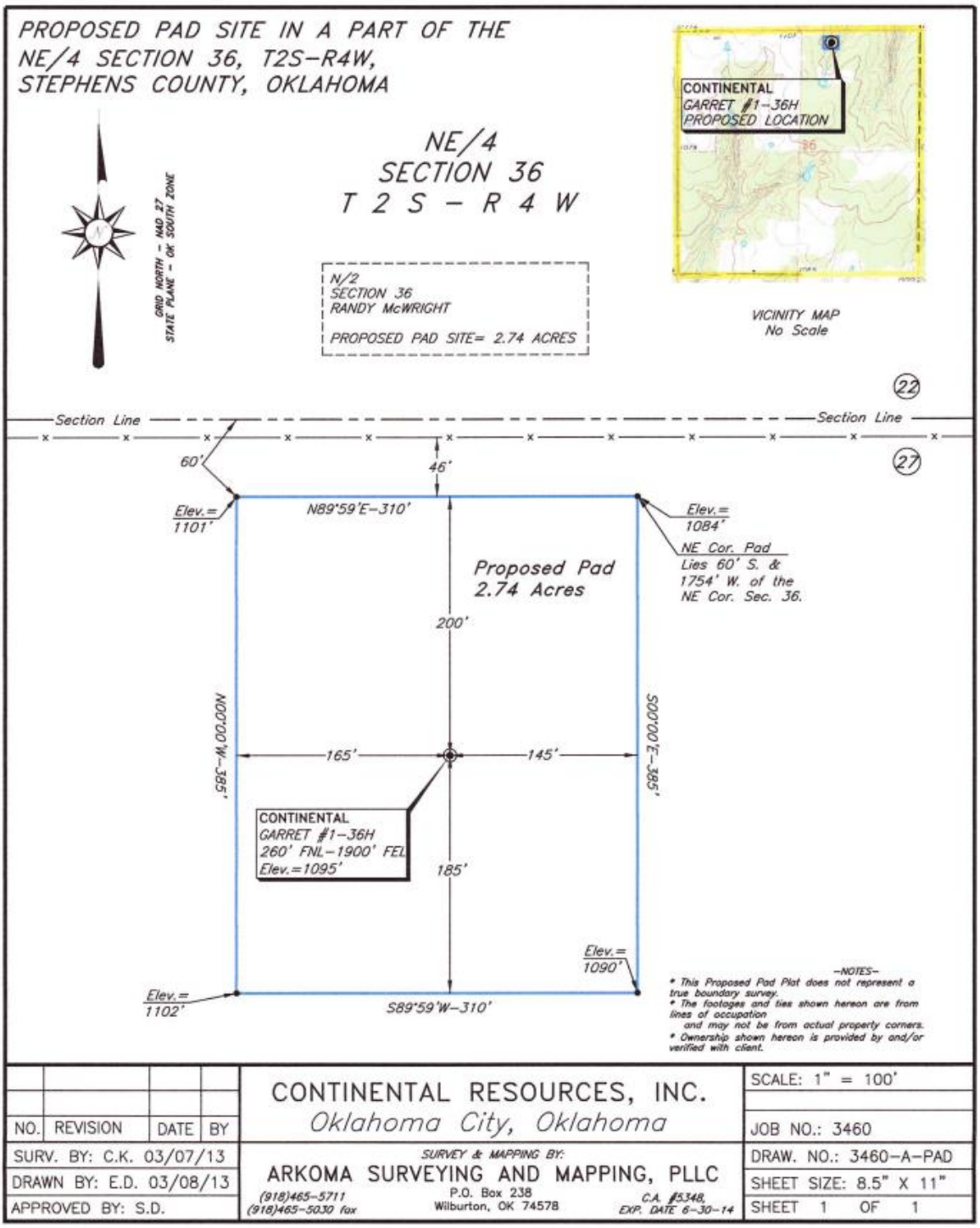

Figure A2: Well Site

GARRETT 1-36H

API #:	3513727134	**County:**	STEPHENS (OK)	**Township:**	02S	**Last Completion Date:**	03-11-2014
Operator:	CONTINENTAL RESOURCES	**Lat, Lon:**	34.3463979, -97.5689999	**Range:**	04W	**Wellbore Count:**	1
Status:	ACTIVE	**Field:**	UNKNOWN	**Q/Q:**	NENW		
Completion Type:	OIL	**Survey:**		**Spud Date:**	12-01-2013		
GL:	1,095 ft	**Section:**	36	**First Completion Date:**	03-11-2014		

PERMITS

PERMIT # 911025

GENERAL

Operator:	CONTINENTAL RESOURCES	**Lease Name:**	GARRETT	**Address:** PAM COMBEST PO BOX 269000 OKLAHOMA CITY, OK 73126		**Filing Purpose:**	NewDrill
TD:	18,930 ft	**Received:**	11-22-2013	**Issued:**	11-22-2013	**RRC Lease ID #:**	0
Phone:	4052349020	**Type:**	H				

SURFACE LOCATION & ACREAGE

District:		**Section:**	36	**Survey:**		**County:**	STEPHENS
Block:		**Abstract:**					

FIELD

Field Name:	NOT REPORTED	**Permit Type:**	OIL

WELLBORES

API # 351372713400

WELLBORE

API #:	351372713400	**Formation:**	WOODFORD	**True Vert. Depth:**	14,211 ft	**Horizontal Length:**	4,980 ft
Trajectory:	H	**Total Depth:**	17,156 ft	**Lateral Length:**	2,695 ft	**Elevation:**	1,095 ft

Figure A3: Well card details 1

API #	Casing Type	Casing Size (in)	Top Depth (ft)	Bottom Depth (ft)	Hole Size (in)	Casing Weight (lb/ft)	Casing Grade	Slurry Volume (cu ft)	Cement Amount (sacks)	Cement Class	Cement Top (ft)
35137271340000	CONDUCTOR CASING	20		86					9		
35137271340000	SURFACE CASING	13.375		1,520		54.5	J-55		930		
35137271340000	INTERMEDIATE CASING	9.625	25	9,975		40	P-110		3,087		25
35137271340000	PRODUCTION CASING	5.5	10,772	17,156		23	P-110		1,525		10,772

Producing Entity:	WELL	**Max Active Wells:**	1	**Cumulative Gas:**	818,968	**Oil EUR:**	
Reservoir:	WOODFORD	**First Prod Date:**	03-01-2014	**Peak Oil:**	3,731	**Gas EUR:**	
District:		**Last Prod Date:**	07-01-2019	**Peak Gas:**	16,959	**Oil Gatherer:**	SUNOCO PARTNERS MKT & TERMINAL
Lease:	GARRETT	**Months Producing:**	65	**Daily Oil:**	43	**Gas Gatherer:**	ENABLE GATHERING & PROCESSING LLC
Latest Well Count:	1	**Cumulative Oil:**	141,606	**Daily Gas:**	366		

Figure A4: Well card details 2

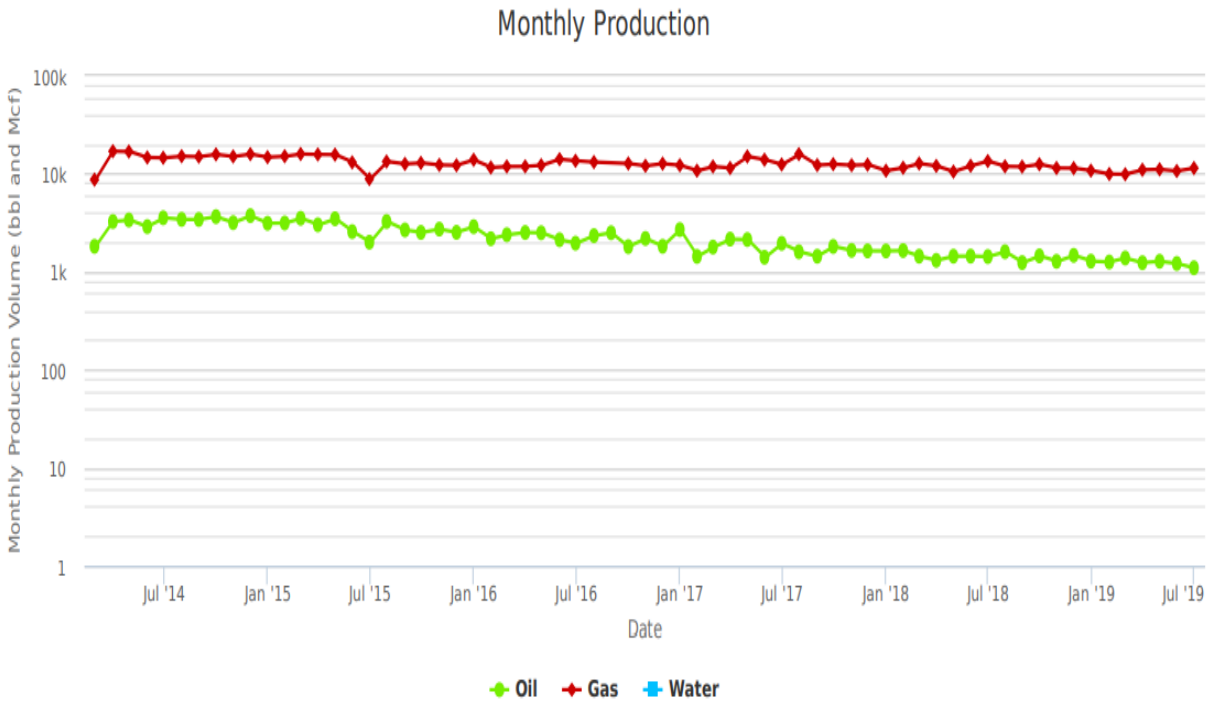

Figure A5: Monthly Production of the Garrett Well

Table A1: Garrett Bit Details

State	County	API #	Well Nbr	Permit No	Type of Well	Project	Ops Project	Section	Township	Range
OKLAHOMA	STEPHENS	35137271340000	212484	13727134	OIL	LOCO	LOCO	36	002S	004W

Well Spud Date	KB Elevation (ft)	Ground Elevation (ft)	Total Measured Depth (ftKB)	PB Depth (ftKB)	TVD (ftKB)
11/30/2013 18:00	1114	1089	17,156.0	Sidetrack 1 - 17,058.0	Sidetrack 1 - 14,212.7

Bits

BHA #	Bit Run	Size (in)	Make	Model	SN	IADC Codes	TFA (incl Noz) (in²)	Nozzles (1/32")	Depth In (ftKB)	Depth Out (ftKB)	Drilled (ft)	Drill Time (hr)	BHA ROP (ft/hr)	WOB Max (1000lbf)	WOB Min (1000lbf)	Max RPM (rpm)	Min RPM (rpm)	Bit Dull
1	1	17 1/2	Baker Hughes	HC6055	7028117	___	0.77	12/12/12/12/12/12/12	86.0	1,520.0	1,434.00	13.50	106.2	12	12	90	60	1-1-NO-A-X-0-NO-TD
2	2	12 1/4	Baker Hughes	DP507X	7146574	M423	1.37	16/16/16/16/16/16/16	1,520.0	4,722.0	3,202.00	84.00	38.1	15	9	140	65	0-0-NO-A-X-0-NO-BHA
3	3	12 1/4	Smith	MSI716MPX	JF3038	M323	1.37	16/16/16/16/16/16/16	4,722.0	5,982.0	1,260.00	35.50	35.5	15	10	184	118	0-1-WT-S-X-0-NO-DTF
4	4	12 1/4	Smith	MSI716MPX	JF5023	M323	1.37	16/16/16/16/16/16/16	5,982.0	8,398.0	2,416.00	99.50	24.3	25	10	184	124	1-2-WT-S-X-0-CT-PR
5	5	12 1/4	Security	MM64D	12266948	___	1.49	18/18/18/18/18/18	8,384.0	9,071.0	687.00	59.50	11.5	24	18	180	120	1-3-WT-S-X-0-CT-PR
6	6	12 1/4	Smith	MSI716MPX	JH3104	M323	1.37	16/16/16/16/16/16/16	9,071.0	9,975.0	904.00	92.00	9.8	20	12	181	121	2-2-BT-N-X-0-WT-TD
7	7	12 1/4	PDC Logic	MD28MBH	H03631	___	0.98	20/20/22	9,975.0	9,975.0								1-1-WT-A-1-0-NO-TD
8	8	8 3/4	Smith	MDSi713MEPX	JH1722	___	0.85	12/12/12/12/12/14/14	9,975.0	9,985.0	10.00	0.50	20.0	8	8	80	80	1-1-BT-C-X-0-CT-HP
9									9,985.0	9,985.0								-------
10	9	8 3/4	Smith	XR+PS	RA1828	___	0.75	18/18/18	9,985.0	9,990.0	5.00	1.00	5.0	28	28	60	60	1-1-WT-A-0-0-NO-BHA
11	10	8 3/4	Smith	MDSi713MEPX	JG4891	___	0.85	12/12/12/12/12/14/14	9,990.0	10,000.0	10.00	2.50	4.0	45	45	60	60	3-3-LT-A-X-0-BT-BHA
12	RR 9	8 3/4	Smith	XR+PS	RA1828	___			10,000.0	10,030.0	30.00	4.50	6.7	20	20	65	65	1-1-WT-A-0-0-NO-BHA
13	11	8 3/4	Security	MMD75DC	12266955	M423	0.85	12/12/12/12/12/14/14	10,030.0	10,848.0	818.00	35.00	23.4	34	12	80	60	0-0-NO-A-x-0-NO-DMF
14	12	8 3/4	Security	MMD75DC	12269261	M432	0.85	12/12/12/12/12/14/14	10,848.0	12,173.0	1,325.00	44.50	29.8	32	20	80	60	0-0-NO-A-X-0-NO-DMF
15	13	8 3/4	Smith	MDSi813MUPXG	JH3735	M 432	0.85	12/12/12/12/12/11/11	12,173.0	12,573.0	400.00	32.00	12.5	38	20	80	80	1-2-WT-A-X-0-FC-PR
16	14	8 3/4	Smith	XR+	RA1828	137	0.85	14/14/12/12/12/12/12	12,573.0	13,065.0	492.00	29.00	17.0	30	25	80	80	1-1-NO-A-X-0-NO-TD
17	RR#9	8 3/4	Smith	XR+	RA1828	137	0.75	18/18/18										1-1-WT-A-0-0-WT-BHA
18	15	8 3/4	Smith	FHI28ODVPS	PY3346	527Y	0.75	18/18/18	10,911.0	11,510.0	599.00	56.50	10.6	70	30	141	121	1-2-BT-G-1-0-WT-BHA
19	16	8 1/2	Smith	MDSi713UBPX	JF1699	___	0.67	11/11/11/11/11/11/12	11,510.0	17,156.0	5,646.00	119.00	47.4	20	12	150	140	1-1-WT-A-X-0-NO-TD

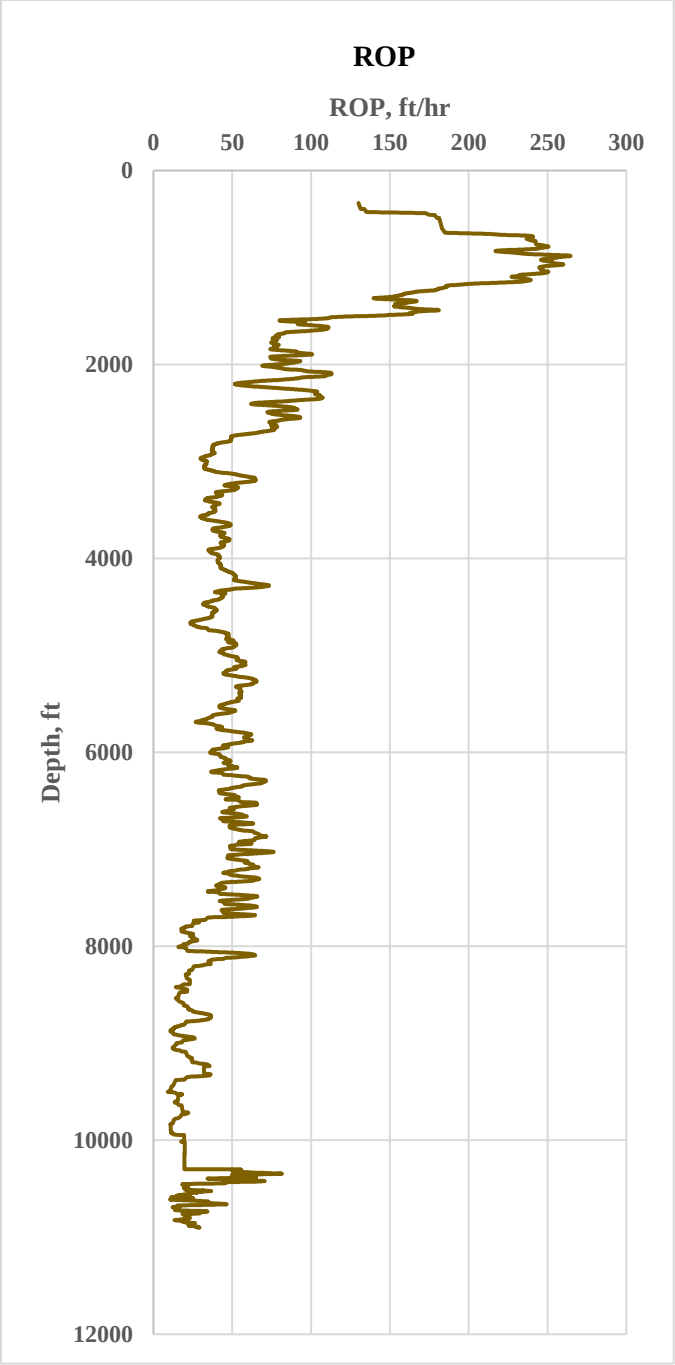

Figure A6: Garrett Input ROP

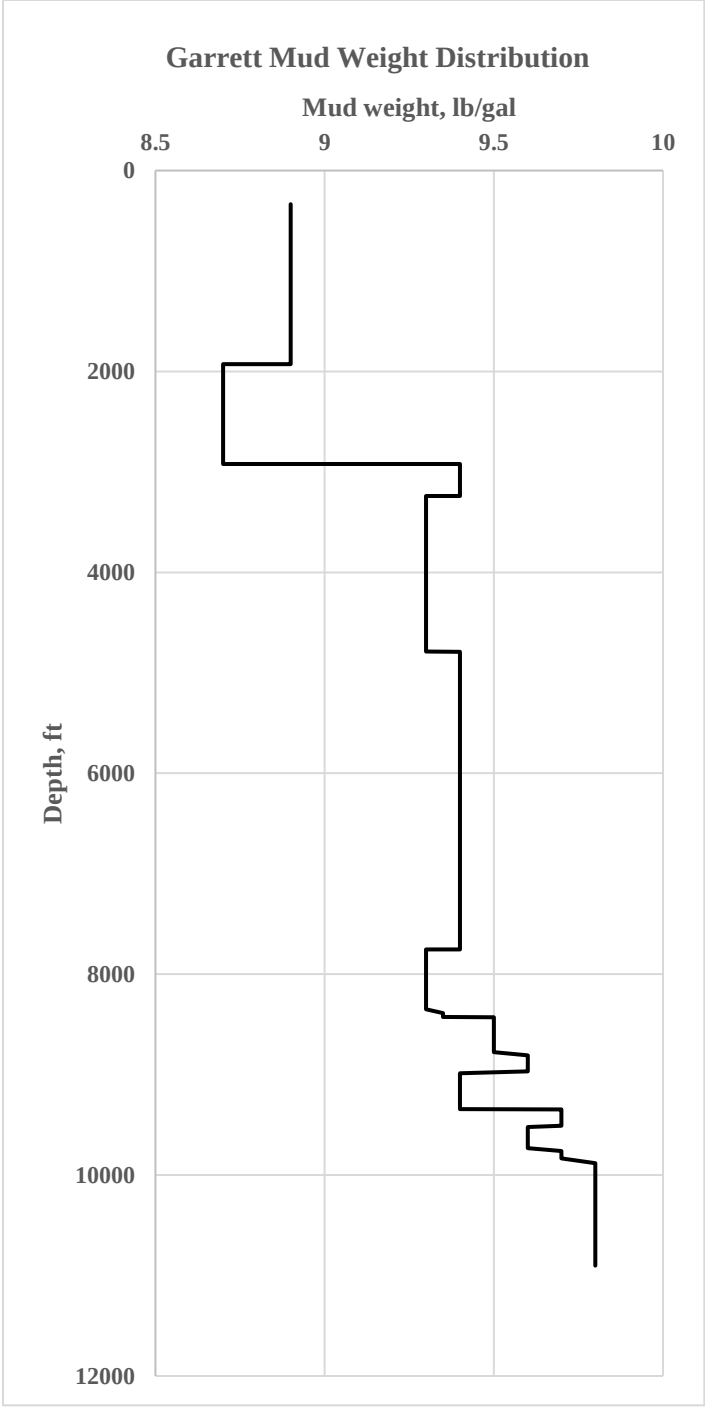

Figure A7: Garrett Mud Weight

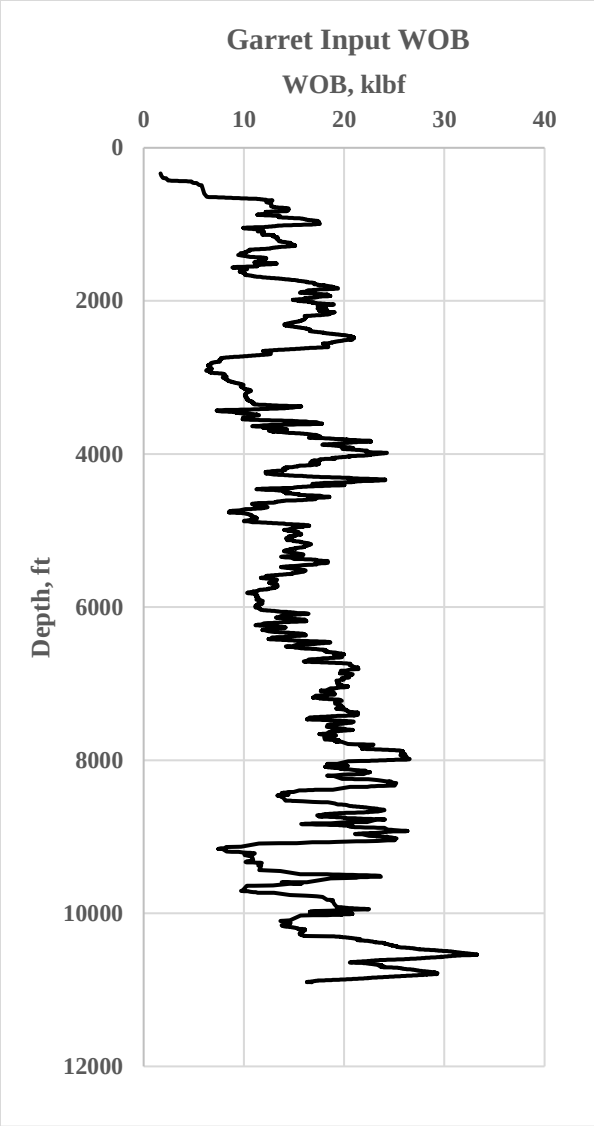

Figure A8: Garrett Input WOB

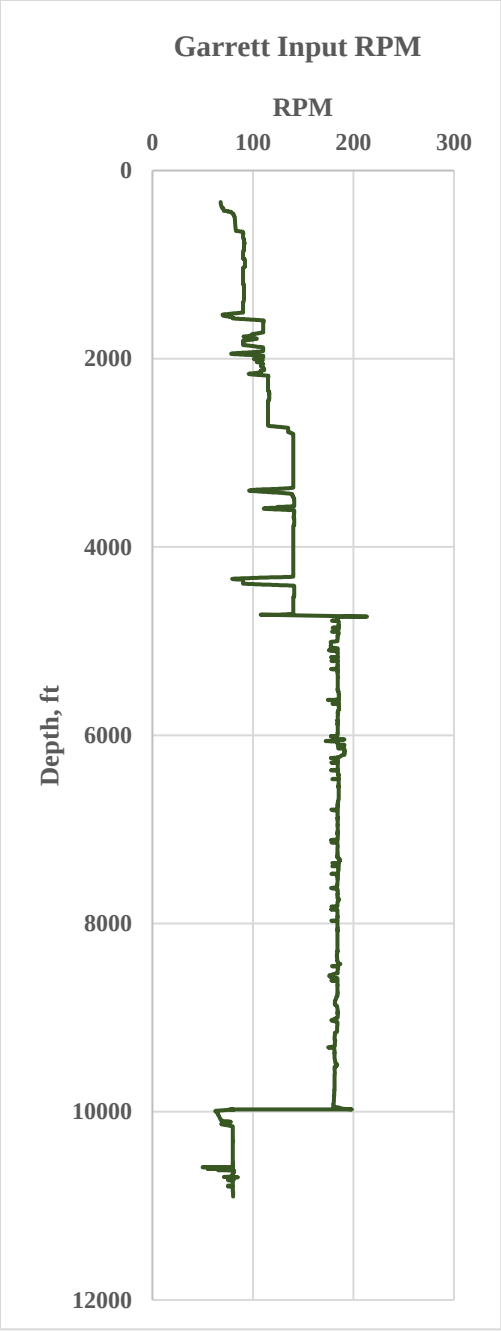

Figure A9: Garrett Input RPM

VITA

Dionne Nyasha Mayibeki

Candidate for the Degree of

Master of Science

Thesis: DRILLING OPTIMIZATION OF A CANEY SHALE WELL USING OFFSET WELL DRILLING DATA

Major Field: Petroleum Engineering

Biographical:

Education:

Completed the requirements for the Master of Science in Petroleum Engineering at Oklahoma State University, Stillwater, Oklahoma in December, 2021.

Completed the requirements for the Bachelor of Science in Chemical Engineering at Oklahoma State University, Stillwater, Oklahoma in 2019.

Professional Memberships:

Society of Petroleum Engineers
American Association of Drilling Engineers
American Society of Chemical Engineers